Commun Nonlinear Sci Numer Simulat 130 (2024) 107725

Contents lists available at ScienceDirect

Communications in Nonlinear Science and Numerical Simulation

journal homepage: www.elsevier.com/locate/cnsns

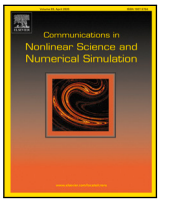

Research paper

Models and numerical methods for XVA pricing under mean reversion spreads in a multicurrency framework

Íñigo Arregui[1], Roberta Simonella[1], Carlos Vázquez [*,1]

Department of Mathematics, University of A Coruña, Campus de Elviña, 15071 A Coruña, Spain
CITIC, Campus de Elviña, 15071 A Coruña, Spain

ARTICLE INFO

Keywords:
XVA
Multicurrency setting
Financial derivatives
Mean reversion processes
(non)linear PDEs
Lagrange-Galerkin method
Monte Carlo techniques
Multilevel Picard iteration

ABSTRACT

In this article we make some new relevant contributions to the computation of total valuation adjustments (XVA) for financial derivatives involving several currencies. From the modelling point of view, for the credit spreads we consider the more realistic exponential Vasicek and CIR positive mean reversion processes. Moreover, the derivative is partially collateralized in cash in a foreign currency and the collateral value is a percentage of the derivative prices. Under this modelling assumptions and using appropriate dynamic hedging methodologies, we obtain formulations in terms of linear and nonlinear partial differential equations, which are solved with Lagrange-Galerkin methods in low dimension. For higher dimensions, we use the Monte Carlo techniques for the equivalent formulations in terms of expectations. These techniques include a multilevel Picard iteration method for the nonlinear case. Finally, the methodologies are applied to several European options with different payoffs and the numerical results are discussed.

1. Introduction

The consideration of the so-called valuation adjustments in the pricing of financial derivatives, motivated by the financial crisis started in 2007, aims to take into account the presence of counterparty risk associated to the different parts in the trade. The set of all these adjustments is usually referred to as XVA (X-Valuation Adjustments) or total valuation adjustment, where "X" can represent any of the first letters in the value adjustments associated to credit (CVA), debit (DVA), funding (FVA), collateral (CollVA), capital (KVA) or margin (MVA), for example. The initial and more classical adjustments are the CVA, FVA and CollVA, while KVA and MVA have been recently added. Among the classical and more general references in the literature, we address the readers to [1–3].

The research work related to XVA has mainly focused on the single currency setting. A first approach aims to obtain formulations based on partial differential equations (PDEs) by means of hedging arguments and the application of Itô's lemma for jump-diffusion processes (see [4–8], for example). A second approach follows the initial ideas in [9] to obtain the CVA by means of formulations based on expectations, next extended to the presence of collateral and funding costs in [10]. This approach has been addressed in [6,11–13], for example. A third approach based on backward stochastic differential equations has been introduced in [14,15].

As a consequence of a fully interconnected worldwide financial sector, not only specially global financial institutions but actually most of them operate in different currencies. For example, in the market they trade on derivatives with underlying assets denominated in different currencies, although if they are denominated in a domestic currency the funding or posting collateral can be done in different foreign currencies. All these real market situations motivated the recent interest in modelling and computing

* Corresponding author at: Department of Mathematics, University of A Coruña, Campus de Elviña, 15071 A Coruña, Spain.
E-mail address: carlosv@udc.es (C. Vázquez).

[1] All authors contributed to all developments and steps of the article.

https://doi.org/10.1016/j.cnsns.2023.107725
Received 7 August 2023; Received in revised form 13 November 2023; Accepted 20 November 2023
Available online 29 November 2023

the XVA in a multi-currency setting. The previously indicated methodologies that have been developed for computing the total valuation adjustments in the single currency case can be extended to the multi-currency one (see [16], for example).

In the present work, we address European options pricing problems in a multi-currency setting when taking into account the valuation adjustments associated to counterparty risk. Thus, we consider a derivative written on different underlying assets that are denominated in different currencies. We consider a zero default intensity for the hedger and a stochastic default intensity (which is equivalent to stochastic credit spread) for the counterparty.

In some sense, we follow our recent articles [17,18], where we deduced the formulations based on PDEs and expectations, only using the second ones for the computation of XVA with Monte Carlo techniques. However, some relevant differences concerning to several more realistic modelling assumptions will be considered in the present article. Also, the numerical solution of the formulation in terms of PDEs for small dimensions will be addressed (see [11], for example) and the use of the much more efficient multilevel Picard iteration technique [19] will be applied for the nonlinear formulations based on expectations. More precisely, note that in our previous work [17] we have chosen a Gaussian dynamics for the credit spread of the counterparty, but this modelling assumption suffers from the possibility of reaching negative credit spread values with positive probability. Unlike this previous work, in this article we consider a more realistic assumption on the credit spread dynamics by choosing positive mean-reversion processes, either an exponential Vasicek or a CIR process. Additionally, this choice allows to borrow calibrated parameters from the literature. Secondly, unlike [17] where the derivative was collateralized partially in bonds and in cash, in the present work we consider the more realistic assumption that the derivative is partially collateralized in cash in a foreign currency and the collateral account value is equal to a percentage of the derivative value. Following the ideas in [18], in a future work we will extend the present article to stochastic foreign exchange (FX) rates.

In the present article, following some ideas in [16], we start building a multi-currency framework where the joint consideration of CVA, FVA, and CollVA are taken into account. Next, we consider suitable hedging arguments and, by applying Itô's formula for jump diffusion processes, we obtain formulations of the derivative pricing problem in terms of PDEs. In order to pose the PDEs formulations for the XVA price, we note that the risky derivative value is obtained by summing the total value adjustment to the derivative risk-free value, i.e., the value that the derivative would have in absence of counterparty risk. Therefore, the XVA can be seen as the difference between the risky derivative value and the risk-free derivative value, that satisfies the classical multidimensional Black–Scholes equation. This allows to obtain a PDE problem for the total value adjustment. Depending on the choice of the mark-to-market value of the derivative at default, different kinds of XVA pricing PDEs arise: if the mark-to-market value is equal to the risky derivative value, then a nonlinear PDE is obtained; if the mark-to-market value is equal to the risk-free derivative value, then a linear PDE that involves the risk-free value of the derivative is deduced.

As the presence of many stochastic factors makes the classical deterministic numerical methods for solving PDEs to be affected by the *curse of dimensionality*, we address the solution of the pricing PDEs using a Lagrange-Galerkin deterministic method just when the derivative only depends on two underlying assets and the counterparty's credit spread is a deterministic function of time.

In order to avoid the *curse of dimensionality* when considering the general case with more than two underlying assets and with stochastic counterparty's credit spread, the Feynman–Kac formula can be applied to formulate the XVA problems in terms of expectations, so that Monte Carlo method can be employed. In particular, in the nonlinear case Picard iteration methods are needed to compute the value adjustment. We use both the simple fixed-point method already used in [17] and the multilevel Picard iteration method proposed in [19]. The results obtained with the formulation in terms of expectations are compared with those with a Lagrange-Galerkin method for the PDEs discretization.

All in all, from the modelling point of view we rigorously establish with detailed financial arguments the models for pricing the XVA associated to European derivatives in a multicurrency setting, with a realistic dynamics for credit spreads that incorporates mean reversion properties. Models are mainly based on detailed replicating portfolio arguments. Either based on expectations or PDEs, these complex (and in many cases high dimension) models require the use of appropriate numerical methods. In the presence of two stochastic factors, we propose the use of PDEs formulations and solve them with Lagrange-Galerkin methods. In the case of a larger number of factors, we propose appropriate Monte Carlo techniques, as for example the multilevel Picard iteration to cope with nonlinear models, to avoid the *curse of dimensionality* associated to deterministic methods for solving PDEs formulations. By using these combination of realistic models and efficient numerical techniques we are able to compute the XVA of European options in the presence of counterparty risk in a multicurrency setting.

Although the previous achievements are relevant, some limitations can be pointed out for a better approach to the market practice and will require further developments. Starting from the setting of this article, we plan to add the consideration of additional valuation adjustments, such as capital value adjustment (KVA) and margin value adjustment (MVA), which are included in market practice. From the modelling point of view, the consideration of stochastic of FX rates instead of constant ones is a work in progress by the authors. Actually, as an example of the increasing use of stochastic dynamics for the different involved factors in a multi-currency setting we refer to [20]. Moreover, the dynamics assumed for the different factors may involve local, stochastic or local-stochastic volatility models or jump-diffusion models instead of constant ones. Also related to the case treated in [20], we note that our article addresses the computation of the XVA for each single financial derivative, while in practice a portfolio of derivative trades is considered and also the different netting sets and credit support agreements must be taken into account.

The article is organized as follows. In Section 2 we deduce the mathematical model for pricing XVA based either on nonlinear or linear PDEs. The equivalent model formulated in terms of expectations is also posed. In Section 3, the proposed numerical methods to solve the previous models are developed. First, we describe the proposed Lagrange-Galerkin method to solve both the nonlinear and the linear PDEs when the counterparty's credit spread is a deterministic function of time. Next, we describe the Monte Carlo method and the quadrature formulae to approximate the integral in the XVA formulae. Moreover, we also describe the multilevel

Picard iteration method, as an alternative to solve the formulation based on expectations. In Section 4 we present and analyse the numerical results related to some examples for different choices of the derivative payoff. More precisely, we consider a *spread option*, an *exchange option* and a *sum of call options*. Finally, in Section 5 we point out our main conclusions.

2. Mathematical models for total value adjustment

2.1. Formulation in terms of partial differential equations

In this section, following [6,16] the value of a derivative is modelled by taking into account the valuation adjustments that have to be considered in case of a possible default of the counterparties involved in the deal.

We consider a trade between a non-defaultable hedger and a defaultable counterparty in a multi-currency framework, where a domestic currency D and foreign currencies $C_0, \dots, C_N$ are involved. For $j = 0, \dots, N$, let X_t^{D,C_j} be the FX rate between currencies D and C_j at time t, namely the domestic price at time t of one unit of the foreign currency C_j.

Concerning FX rates, in the present article we assume that they are time dependent and deterministic, satisfying the following differential equation:

$$dX_t^{D,C_j} = (r^D - r^{C_j})X_t^{D,C_j}\,dt, \quad j = 0, \dots, N\,.$$

where r^D and r^{C_j} are the short-term rates in the domestic market and in the $j-$foreign market, respectively. Furthermore, in the numerical examples we consider constant values for X_t^{D,C_j}, so that subindex t will be removed in that section. The extension to stochastic FX rates will be addressed in future work.

We denote by $S_t = (S_t^1, \dots, S_t^N)$ the vector of the prices of the underlying assets S^i at time t, each one of them being denominated in its corresponding currency C_i, and by h_t the counterparty's credit spread at time t. The credit spread of an entity is typically calculated as the difference between the rate of return on a bond issued by the risky entity and the risk-free rate. Therefore, the credit spread gives an indication of the market's view of the riskiness of that bond and of the probability of default of an entity. In fact, the intensity of default λ can be modelled [6] as

$$\lambda \approx \frac{h}{1 - R_C}\,,$$

where R_C is the entity's recovery rate.

We assume that under the real world measure P the evolution of the prices of the underlying assets in each currency and of the counterparty's credit spread are governed by the following SDEs:

$$dS_t^i = \mu^{S^i} S_t^i\,dt + \sigma^{S^i} S_t^i\,dW_t^{S^i,P}, \quad \text{for } i = 1, \dots, N\,, \tag{1}$$

$$dh_t = \mu^{h,P}(t,h_t)\,dt + \sigma^{h,P}(t,h_t)\,dW_t^{h,P}\,, \tag{2}$$

where μ^{S^i} and $\mu^{h,P}$ are the real world drifts of the processes S_t^i and h_t, respectively. Moreover, σ^{S^i} and $\sigma^{h,P}$ are their respective volatility functions, while $W^{S^i,P}$ and $W^{h,P}$ are Brownian motions under the real world measure P. Moreover, we assume that the assets prices and spread processes in (1) and (2) are correlated. For this purpose, we denote the correlation $\rho^{S^iS^j}$ between S^i and S^j, while the correlation between S^i and h is denoted by ρ^{S^ih}. In this work, we consider constant values for correlations.

By changing the probability measure from P to the risk-neutral measure in the domestic currency, Q^D, in (1) we have that the dynamics of S^i, for $i = 1, \dots, N$, is given by

$$dS_t^i = (r^i - q^i)S_t^i\,dt + \sigma^{S^i} S_t^i\,dW_t^{S^i,Q^D}\,,$$

where r^i and q^i are the short-term rate in currency C_i and the dividend paid by S^i, respectively, while W^{S^i,Q^D} is a standard Brownian motion under Q^D.

Note that the drift of the dynamics of S_t^i under Q^D can be obtained from the following arguments.

Let μ^{S^i,Q^D} be the drift of S^i under Q^D, so that the dynamics of S^i under Q^D is given by the SDE:

$$dS_t^i = \mu^{S^i,Q^D} S_t^i dt + \sigma^{S^i} S_t^i dW_t^{S^i,Q^D},$$

so that

$$S_t^i = S_0^i \exp\Big(\Big(\mu^{S^i,Q^D} - \frac{(\sigma^{S^i})^2}{2}\Big)t + \sigma^{S^i} W_t^{S^i,Q^D}\Big).$$

Therefore, the value of the underlying asset S^i in the domestic currency D, denoted by $S^{i,D}$, is given by

$$S_t^{i,D} = S_t^i X_t^{D,C_i} = S_0^{i,D} \exp\Big(\Big(\mu^{S^i,Q^D} - \frac{(\sigma^{S^i})^2}{2} + r^D - r^i\Big)t + \sigma^{S^i} W_t^{S^i,Q^D}\Big).$$

Finally, we obtain

$$dS_t^{i,D} = \Big(\mu^{S^i,Q^D} + r^D - r^i\Big)S_t^{i,D}dt + \sigma^{S^i} S_t^{i,D} dW_t^{S^i,Q^D}.$$

Since the drift of $S^{i,D}$ under Q^D is given by $r^D - q^i$, we get $\mu^{S^i,Q^D} = r^i - q^i$.

Although in the numerical examples we consider constant values for r^i, q^i and for the volatility σ^i, time dependent functions can be assumed in all the developments. Moreover, by changing from P to Q^D in (2), the drift of h is given by $\mu^{h,P} - M^h\sigma^{h,P}$, where M^h is the counterparty's market price of credit risk.

As indicated in [21], the study of historical credit spreads time series suggests that credit spreads exhibit mean reverting and fat tails properties. Therefore, under the risk-neutral measure Q^D, we model the counterparty's credit spread by an exponential Vasicek process, i.e., we assume that the logarithm of h follows a Vasicek dynamics. Thus, we denote by $\tilde{h}$ the logarithm of h and assume

$$d\tilde{h}_t = \alpha\,(\theta - \tilde{h}_t)\,dt + \sigma^h\,dW^{h,Q^D}\,,$$

where α, θ and σ^h are positive constant and W^{h,Q^D} is a Brownian motion under the risk-neutral measure Q^D. In particular, α is the mean reversion rate, θ is the mean reversion level and σ^h is the volatility of the mean reversion process. Then, by applying Itô's formula (see, for example, [22]) to $h_t = \exp(\tilde{h})$, we get

$$dh_t = \alpha\,h_t\,(m - \log(h_t))\,dt + \sigma^h\,h_t\,dW^{h,Q}\,,\ \text{with}\ \ m = \theta + \frac{(\sigma^h)^2}{2\alpha}\,. \tag{3}$$

The exponential transformation ensures the positivity of h.

However, in the literature the credit spread is often assumed to follow a Cox–Ingersoll–Ross (CIR) process, so that the dynamics of h is given by the following mean reverting SDE:

$$dh_t = \alpha\,(\theta - h_t)\,dt + \sigma^h\sqrt{h_t}\,dW^{h,Q^D}\,, \tag{4}$$

where α, θ and σ^h are positive constants and if the Feller condition is fulfilled, i.e., $2\,\alpha\,\theta > (\sigma^h)^2$, then h remains strictly positive. In Section 4, where numerical results are presented, we also report results with CIR dynamics for the credit spread. However, in the development of the mathematical models we only show those obtained with exponential Vasicek dynamics, since it would be redundant to repeat the same steps with only a different dynamics for the credit spread. Note that in [17] we have considered a Normal dynamics for the counterparty's credit spread, and we now consider a more realistic hypothesis by assuming it is modelled by a positive mean-reversion process.

Next, we denote by J_t the counterparty's default state at time t, defined as $J_t = 1$ if the counterparty defaults before or at time t, while $J_t = 0$ otherwise.

The derivative value in the domestic currency D at time t is given by $V_t^D = V^D(t, S_t, h_t, J_t)$. We will refer to this derivative that involves counterparty risk as risky derivative. The price in currency D of the same derivative traded between two non-defaultable counterparties is denoted by $W_t^D = W^D(t, S_t)$. This derivative will be referred to as risk-free derivative price. Note that both derivatives are affected by market risk, so we will use the term "risky" and "risk-free" in terms of credit risk.

We assume the derivative is partially collateralized in cash in the foreign currency C_0. We denote by $C_t^{C_0}$ the collateral account value at time t in currency C_0.

The close-out procedure in case of default event is described in ISDA (International Swaps and Derivatives Association) documentation: if the surviving party is a net debtor, then she must pay the whole close-out value to the defaulting party; if the surviving party is a net creditor, then she is able to recover only a fraction of her credits. We assume that the derivative is traded under the presence of a collateral account. Collateralized contracts are regulated by the Credit Support Annex (CSA) to the ISDA Master Agreement. Therefore, taking into account the presence of the collateral, that has the role to reduce the exposure, the expression of the risky derivative value at default is given by:

$$V^D(t, S_t, h_t, 1) = C^D(t) + R_C\left(M^D(t, S_t, h_t) - C^D(t)\right)^+ + \left(M^D(t, S_t, h_t) - C^D(t)\right)^-\,, \tag{5}$$

with $M^D(t, S_t, h_t)$ representing the mark-to-market derivative price and $C^D(t)$ denoting the collateral account value in domestic currency D. Moreover, we have used the notation $x^+ = \max(x, 0)$ and $x^- = \min(x, 0)$. Eq. (5) means that, in case of counterparty's default:

- if the hedger is a net debtor, i.e., $M^D - C^D \le 0$, then the hedger has to pay the whole mark-to-market derivative value to the counterparty;
- if the hedger is a net creditor, i.e., $M^D - C^D > 0$, then the hedger is able to recover a fraction of her credits, given by $C^D + R_C(M^D - C^D)$.

Note that, since the recovery rate R_C is between 0 and 1, the default payment $C^D + R_C(M^D - C^D)$ is always greater than the default payment it would happen in absence of collateral, that is just given by $R_C M^D$. Therefore, the collateralization improves the recovery in case of counterparty's default.

By using (5), we can define the variation of V^D at default as:

$$\Delta V^D = C^D + R_C(M^D - C^D)^+ + (M^D - C^D)^- - V^D\,, \tag{6}$$

where we have suppressed the dependence on time t, on the underlying assets S_t and on the counterparty's credit spread h_t to ease the notation.

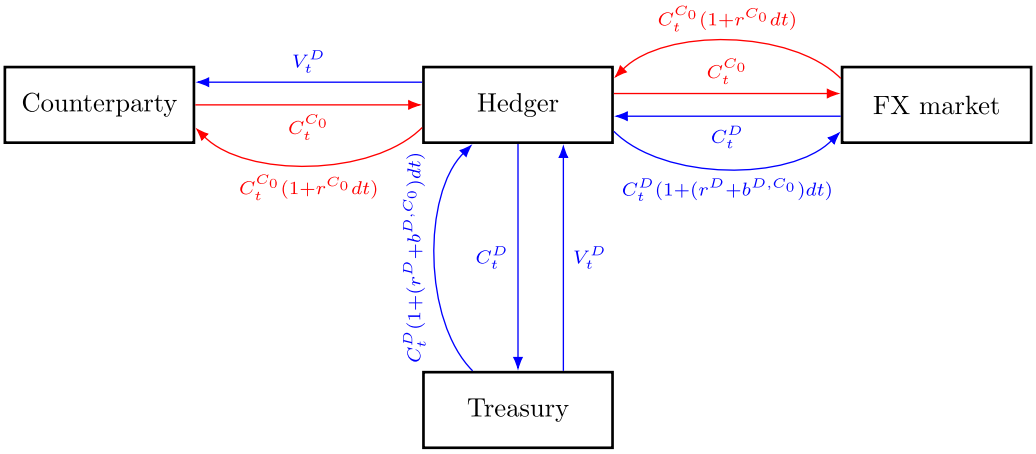

Fig. 1. Transactions occurring with the treasury and the FX market to fund the trade. Straight lines refer to initial transactions, that take place at time t, while curved lines to final transactions taking place at time $t+dt$. Blue lines indicate amounts denominated in currency D, whereas red ones represent cash denominated in currency C_0.

2.2. Replicating portfolio

In order to price the derivative, we consider a self-financing portfolio Π that hedges all the risk factors, which are:

- the market risk due to changes in $S^1, S^2, \dots, S^N$;
- the counterparty's spread risk due to changes in h;
- the counterparty's default risk.

More precisely:

- the market risk due to changes in S^i, for $i = 1, \dots, N$, is hedged by trading in fully cash collateralized derivatives on the same underlying assets. For $i = 1, \dots, N$, the net present value in currency C_i of the derivative written on the underlying asset S^i is denoted by H^i, so that $H^{i,D} = H^i X^{D,C_i}$ represents the net present value of H^i in the currency D;
- in order to hedge the spread risk due to changes in counterparty's credit spread h and the counterparty's default risk, the hedger has to trade in two credit default swaps with different maturities written on the counterparty:
  - a short term credit default swap, $CDS^D(t, t+dt)$, that is an overnight credit default swap with unit notional. The protection buyer pays a premium at time t equal to $h_t dt$ and receives $(1 - R_C)$ at time $t+dt$ if the counterparty defaults between t and $t+dt$. We assume that $h_t dt$ is such that $CDS^D(t, t+dt) = 0$;
  - a long term credit default swap, $CDS^D(t, T)$, that is a cash collateralized credit default swap maturing on T. In general, $CDS^D(t, T)$ is not null.

We now assume that the hedger buys the derivative from the counterparty, with $V_t^D > 0$, and we describe the operations she would enact in a generic small time interval $[t, t+dt]$ with the treasury and the FX market to fund the trade. The transactions are represented in Fig. 1.

- At time t, the hedger borrows V_t^D cash from her bank treasury to buy the derivative from the counterparty and receives the collateral amount $C_t^{C_0}$ in currency C_0.
- The hedger exchanges the cash $C_t^{C_0}$ in the FX spot market, obtaining $C_t^D = C_t^{C_0} X_t^{D,C_0}$, that she gives to the treasury. Therefore, the outstanding debt to the treasury is $V_t^D - C_t^D$, that will grow at the borrowing rate in currency D, denoted by $f_t^{B,D}$.
- At time $t+dt$, the hedger has to pay back the collateral plus interest, given by the OIS rate in currency C_0, denoted by $r_t^{C_0}$. Thus, according to a forward contract agreed at time t, she sells forward the amount $C_t^{C_0}(1+r^{C_0}dt)$ in currency C_0 multiplied by the forward FX rate $X_t^{D,C_0} \frac{1+r^D dt}{1+(r^{C_0}+b^{C_0,D})dt}$ and receives $C_t^{C_0}(1+r^{C_0}dt)$ in currency C_0. The rate r^D is the OIS rate in the domestic currency D, whereas $b^{C_0,D}$ denotes the short term cross-currency basis between currencies C_0 and D, which is an adjustment that needs to be made in the C_0 rate. The hedger pays the amount $C_t^{C_0}(1+r^{C_0}dt)$ to the counterparty.
- At time $t+dt$ the debt to treasury is

$$\left(V_t^D - C_t^D\right)\left(1 + f_t^D dt\right) + C_t^D\left(1 + (r^D + b^{D,C_0})dt\right).$$

Note that in the case $V_t < 0$, the trades would be right the opposite.

We denote by B_t^D the value of the funding account in the domestic currency D at time t and by Ω_t the number of shares of the funding account at time t. Thus, in order to ensure that the self financing condition holds, we have the following funding constraint

condition:

$$\Omega_t B_t^D = -\left(V_t^D - C_t^{C_0} X_t^{D,C_0}\right). \tag{7}$$

Note that if $\Omega_t > 0$, then the hedger has to finance her position by borrowing from the treasury and she will pay an interest rate $f_t^{D,C}$, where C stands for cost. Vice versa, if the hedger's position is positive, she will invest money by lending to the treasury and earning at the rate $f_t^{D,B}$, where B stands for benefit. Therefore, if we define the funding rate in currency D as

$$f_t^D = f_t^{D,C} \mathbb{1}_{\Omega_t > 0} + f_t^{D,B} \mathbb{1}_{\Omega_t < 0}, \tag{8}$$

we have that

$$B_t^D = \exp\left(\int_0^t f_t^D ds\right). \tag{9}$$

Hence, we consider a replicating portfolio Π that is an extension to the multi-currency framework of the portfolio in [8] and such that:

- α_t^i is the weight of the fully collateralized derivative H_t^i, for $i = 1, \dots, N$, in the portfolio composition at time t;
- γ_t and ϵ_t are the weights of the long term CDS and short term CDS, respectively, in the portfolio composition at time t;
- Ω_t represents the number of shares of the funding account at time t;
- β_t^D denotes the cash in the collateral accounts of the portfolio at time t.

Thus, the portfolio at time t is given by:

$$\Pi_t = \sum_{i=1}^N \alpha_t^i H_t^{i,D} + \gamma_t CDS^D(t,T) + \epsilon_t CDS^D(t,t+dt) + \Omega_t B_t^D + \beta_t^D. \tag{10}$$

The composition of the collateral account β^D is given by

$$\beta_t^D = -\sum_{i=1}^N \alpha_t^i H_t^{i,D} - \gamma_t CDS^D(t,T) - C_t^{C_0} X_t^{D,C_0}.$$

In order to infer the variation of the collateral account in the time interval $[t, t+dt]$, we analyse the transactions occurring when trading a generic fully collateralized derivative in a foreign currency F. We denote the value of the foreign derivative by H^F and we again assume the hedger buys the derivative, with $H_t^F > 0$.

- At time t, the hedger borrows $H_t^D = H_t^F X^{D,F}$ cash from her bank treasury, that exchanges in the FX market receiving H_t^F in currency F. Thus, the hedger buys the derivative.
- The hedger receives the collateral with value H_t^F and exchanges this amount in the FX market, getting H_t^D, that she gives back to the treasury.
- At time $t + dt$ the hedger has to give back the collateral plus interest, given by the OIS rate in currency F, r_t^F. Therefore, at time t the hedger agrees to exchange forward in the FX market the amount $H_t^F(1 + r^F dt)$ in currency F multiplied by the forward FX rate $X_t^{D,F} \frac{1+r^D dt}{1+(r^F + b^{F,D})dt}$, where $b^{F,D}$ is the cross-currency basis between currency F and currency D, and receives $H_t^F(1 + r^F dt)$ in currency F. The hedger pays this amount to the counterparty. The variation in the collateral account is given by

$$H_t^D\left(1 + (r^D + b^{D,F})dt\right).$$

Therefore, from Figs. 1 and 2 we infer that the variation of the collateral account in the time interval $[t, t+dt]$ is given by:

$$d\bar{\beta}_t^D = \left[-\sum_{i=1}^N \alpha_t^i (r^D + b^{D,C_i}) H_t^{i,D} - \gamma_t r^D CDS^D(t,T) - \left(r^D + b^{D,C_0}\right) C_t^{C_0} X_t^{D,C_0}\right] dt,$$

where b^{D,C_j}, for $j = 0, \dots, N$, is the cross-currency basis between the domestic currency D and the foreign currency C_j.

2.3. Pricing partial differential equations

Once we have built our replicating portfolio, we consider the no arbitrage and the self-financing conditions to infer the pricing PDEs. Therefore, we have

$$\Pi(t) + V^D(t, S_t, h_t, J_t) = 0,$$

thus:

$$\begin{aligned} -dV_t^D &= d\Pi_t \\ &= \sum_{i=1}^N \alpha_t^i dH_t^{i,D} + \gamma_t dCDS^D(t,T) + \epsilon_t dCDS^D(t,t+dt) + \Omega_t dB^D + d\bar{\beta}_t^D. \end{aligned} \tag{11}$$

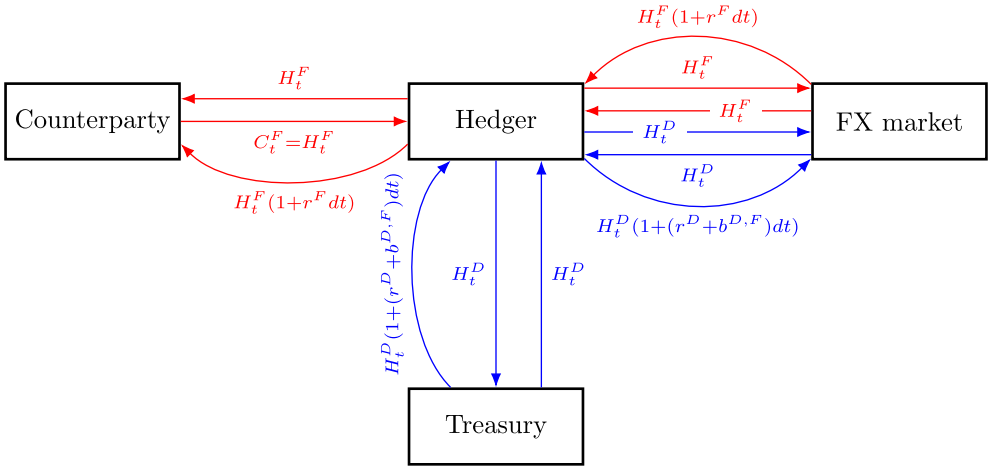

Fig. 2. Transactions occurring when trading a fully collateralized foreign derivative. Straight lines refer to initial transactions, that take place at time t, while curved lines to final transactions taking place at time $t + dt$. Blue lines indicate amounts denominated in the domestic currency D, whereas red ones represent cash denominated in the foreign currency F.

As $V_t^D = V^D(t, S_t, h_t, J_t)$ depends on diffusion and jump processes, we apply Itô's formula for jump-diffusion processes [22] to obtain that the variation of V^D in the time interval $[t, t + dt]$ is given by:

$$\begin{aligned} dV_t^D &= \frac{\partial V^D}{\partial t}dt + \sum_{i=1}^{N}\frac{\partial V^D}{\partial S^i}dS_t^i + \frac{\partial V^D}{\partial h}dh_t + \Delta V_t^D dJ_t \\ &+ \left[\frac{1}{2}\sum_{i,k=1}^{N}\rho^{S^iS^k}\sigma^{S^i}\sigma^{S^k}S_t^iS_t^k\frac{\partial^2 V^D}{\partial S^i\partial S^k}\right. \\ &\left. + \frac{1}{2}(\sigma^h h_t)^2\frac{\partial^2 V^D}{\partial h} + \sum_{i=1}^{N}\rho^{S^ih}\sigma^{S^i}\sigma^h S_t^i h_t\frac{\partial^2 V^D}{\partial S^i\partial h}\right]dt, \end{aligned}$$

where $\Delta V_t^D = V^D(t, S_t, h_t, 1) - V^D(t, S_t, h_t, 0)$ represents the jump of V_t^D in case of default at time t, which is given by (6).

The dynamics of the short term credit default swap, $CDS^D(t, t + dt)$, and of the funding account, B_t^D, are respectively given by:

$$dCDS^D(t, t + dt) = h_t\,dt - (1 - R_C)\,dJ_t, \tag{12}$$

$$dB_t^D = f^D B_t^D\,dt. \tag{13}$$

From the funding condition on our strategy, stated in (7), we obtain

$$\Omega_t = -\frac{V_t^D - C_t^D}{B_t^D}.$$

Thus, the change in Π_t from t to $t + dt$ is given by:

$$\begin{aligned} d\Pi_t &= \sum_{i=1}^{N}\alpha_t^i dH_t^{i,D} + \gamma_t dCDS^D(t,T) + \epsilon_t dCDS^D(t,t+dt) \\ &\quad - \frac{V_t^D - C_t^{C_0}X_t^{D,C_0}}{B_t^D}dB_t^D + d\bar{\beta}_t^D \\ &= \sum_{i=1}^{N}\alpha_t^i\left(\frac{\partial H^{i,D}}{\partial t}dt + \frac{\partial H^{i,D}}{\partial S^i}dS_t^i + \frac{1}{2}(\sigma^{S^i}S_t^i)^2\frac{\partial^2 H^{i,D}}{\partial (S^i)^2}dt\right) \\ &\quad + \gamma_t\left[\frac{\partial CDS^D(t,T)}{\partial t}dt + \frac{\partial CDS^D(t,T)}{\partial h}dh_t + \frac{1}{2}(\sigma^h h)^2\frac{\partial^2 CDS^D(t,T)}{\partial h^2}dt\right] \\ &\quad + \gamma_t\Delta CDS^D(t,T)dJ_t + \epsilon_t\left[h_t dt - (1-R_C)dJ_t\right] - (V^D - C_t^{C_0}X_t^{D,C_0})f^D dt \\ &\quad - \sum_{i=1}^{N}\alpha_t^i(r^D + b^{D,C_i})H_t^{i,D}dt - \gamma_t r^D CDS^D(t,T)dt - (r^D + b^{D,C_0})C_t^{C_0}X_t^{D,C_0}dt. \end{aligned}$$

In order to hedge the risk of the portfolio Π, we choose:

$$\alpha_t^i = -\frac{\partial V^D/\partial S^i}{\partial H^{i,D}/\partial S^i}, \quad \text{for } i = 1, \dots, N,$$

$$\gamma_t = -\frac{\partial V^D/\partial h}{\partial CDS^D(t,T)/\partial h}, \qquad \epsilon_t = \frac{1}{1-R_C}\left(\gamma_t \Delta CDS^D(t,T) + \Delta V^D\right).$$

Next, we take into account the Black–Scholes equations that model $H^{i,D}$ and $CDS^D(t,T)$, namely

$$\begin{aligned}
&\frac{\partial H^{i,D}}{\partial t} + \frac{1}{2}(\sigma^{S^i} S^i)^2 \frac{\partial^2 H^{i,D}}{\partial (S^i)^2} + (r^i - q^i) S^i \frac{\partial H^{i,D}}{\partial S^i} = (r^D + b^{D,C_i}) H^{i,D},\\
&\frac{\partial CDS^D(t,T)}{\partial t} + \frac{1}{2}(\sigma^h h)^2 \frac{\partial CDS^D(t,T)}{\partial h^2} + (\mu^{h,P} - M^h \sigma^{h,P}) \frac{\partial CDS^D(t,T)}{\partial h}\\
&\qquad + \frac{h}{1-R_C} \Delta CDS^D(t,T) = r^D CDS^D(t,T).
\end{aligned}$$

Thus, (11) turns into:

$$\begin{aligned}
&\frac{\partial V^D}{\partial t} + \sum_{i=1}^N \frac{\partial V^D}{\partial S^i}(r^i - q^i) S^i + \frac{\partial V^D}{\partial h}(\mu^h - M^h \sigma^h)\\
&\qquad + \frac{1}{2}\sum_{i,k=1}^N \rho^{S^i S^k} \sigma^{S^i} \sigma^{S^k} S^i S^k \frac{\partial^2 V^D}{\partial S^i \partial S^k} + \frac{1}{2}(\sigma^h h)^2 \frac{\partial^2 V^D}{\partial h^2} + \sum_{i=1}^N \rho^{S^i h} \sigma^{S^i} \sigma^h S^i \frac{\partial^2 V^D}{\partial S^i \partial h}\\
&= -\frac{h}{1-R_C} \Delta V^D + f^D V^D + (r^D + b^{D,C_0} - f^D) C^{C_0} X^{D,C_0}.
\end{aligned}$$

Therefore, we obtain the following pricing PDE:

$$\frac{\partial V^D}{\partial t} + \mathcal{L}_{Sh} V^D - f^D V^D + \frac{h}{1-R_C} \Delta V^D = (r^D + b^{D,C_0} - f^D) C^{C_0} X^{D,C_0}, \tag{14}$$

where the second order differential operator $\mathcal{L}_{Sh}$ is given by

$$\begin{aligned}
\mathcal{L}_{Sh} &= \frac{1}{2}\sum_{i,k=1}^N \rho^{S^i S^k} \sigma^{S^i} \sigma^{S^k} S^i S^k \frac{\partial^2}{\partial S^i \partial S^k} + \frac{1}{2}(\sigma^h h)^2 \frac{\partial^2}{\partial h^2}\\
&+ \sum_{i=1}^N \rho^{S^i h} \sigma^{S^i} \sigma^h S^i \frac{\partial^2}{\partial S^i \partial h} + \sum_{i=1}^N (r^i - q^i) S^i \frac{\partial}{\partial S^i} + (\mu^h - M^h \sigma^h) \frac{\partial}{\partial h}.
\end{aligned} \tag{15}$$

Finally, we use the Q-drift of h given in (3) to write the differential operator (15) as follows:

$$\begin{aligned}
\mathcal{L}_{Sh} &= \frac{1}{2}\sum_{i,k=1}^N \rho^{S^i S^k} \sigma^{S^i} \sigma^{S^k} S^i S^k \frac{\partial^2}{\partial S^i \partial S^k} + \frac{1}{2}(\sigma^h h)^2 \frac{\partial^2}{\partial h^2}\\
&+ \sum_{i=1}^N \rho^{S^i h} \sigma^{S^i} \sigma^h S^i \frac{\partial^2}{\partial S^i \partial h} + \sum_{i=1}^N (r^i - q^i) S^i \frac{\partial}{\partial S^i} + \alpha h (m - \log(h)) \frac{\partial}{\partial h}.
\end{aligned} \tag{16}$$

In the pricing equation (14) the variation of V^D upon default is involved and is given by (see (6)):

$$\Delta V_t^D = C_t^D + R_C (M_t^D - C_t^D)^+ + (M_t^D - C_t^D)^- - V_t^D.$$

Following the seminal article [5], in the literature two possible values for the mark-to-market at default, M^D, can be chosen: either equal to the risky value or to the risk-free value of the derivative. Thus, we derive the following PDEs for both cases.

- If $M^D = V^D$, the variation of V^D upon default is given by:

$$\begin{aligned}
\Delta V^D &= C^D + R_C (V^D - C^D)^+ + (V^D - C^D)^- - V^D\\
&= -(1 - R_C)(V_t^D - C_t^D)^+,
\end{aligned}$$

  so that (14) turns into

$$\frac{\partial V^D}{\partial t} + \mathcal{L}_{Sh} V^D - f^D V^D = h (V^D - C^D)^+ + (r^D + b^{D,C_0} - f^D) C^D. \tag{17}$$

- If $M^D = W^D$, the variation of V^D upon default is given by:

$$\begin{aligned}
\Delta V^D &= C^D + R_C (W^D - C^D)^+ + (W^D - C^D)^- - V^D\\
&= W^D - V^D - (1 - R_C)(W^D - C^D)^+,
\end{aligned}$$

  so that (14) becomes

$$\begin{aligned}
&\frac{\partial V^D}{\partial t} + \mathcal{L}_{Sh} V^D - \left(\frac{h}{1-R_C} + f^D\right) V^D\\
&\quad = h (W^D - C^D)^+ - \frac{h}{1-R_C} W^D + (r^D + b^{D,C_0} - f^D) C^D.
\end{aligned} \tag{18}$$

Next, in order to pose the PDEs formulation for the XVA price, the risky derivative value can be split up into $V^D = W^D + U$, where W^D and U represent the risk-free derivative price and the XVA price, respectively.

Note that the risk-free derivative price W^D satisfies the classical Black–Scholes equation:

$$\begin{cases} \partial_t W^D + \mathcal{L}_S W^D - f^D W^D = 0\,, \\ W^D(T,S) = G(S)\,, \end{cases} \tag{19}$$

where $G = G(S)$ is the payoff function and

$$\mathcal{L}_S = \frac{1}{2}\sum_{i,k=1}^{N} \rho^{S^i S^k}\sigma^{S^i}\sigma^{S^k} S^i S^k \frac{\partial^2}{\partial S^i \partial S^k} + \sum_{i=1}^{N}(r^i - q^i)S^i \frac{\partial}{\partial S^i}\,. \tag{20}$$

Moreover, since the final conditions for V^D and for W^D coincide, i.e.,

$$W^D(T,S) = V^D(T,S,h) = G(S)\,,$$

the final condition for U is given by $U(T,S,h) = 0$.

Therefore, depending on the choice of the mark-to-market value at default we obtain two possible PDE problems satisfied by the XVA.

- Nonlinear final value problem (case $M = V^D$):

$$\begin{cases} \dfrac{\partial U}{\partial t} + \mathcal{L}_{Sh} U - f^D U = h(W^D + U - C^D)^+ + (r^D + b^{D,C_0} - f^D)C^D\,, \\ U(T,S,h) = 0\,. \end{cases} \tag{21}$$

- Linear final value problem (case $M = W^D$):

$$\begin{cases} \dfrac{\partial U}{\partial t} + \mathcal{L}_{Sh} U - \left(\dfrac{h}{1-R_C} + f^D\right) U = h(W^D - C^D)^+ + (r^D + b^{D,C_0} - f^D)C^D\,, \\ U(T,S,h) = 0\,. \end{cases} \tag{22}$$

In both cases, $(t,S,h) \in [0,T)\times(0,+\infty)^N \times (0,+\infty)$.

Note that the spatial dimension of problems (21) and (22) depends on the number of underlying assets, so that the PDE easily becomes high dimensional in space and the numerical solution requires specific discretization techniques to overcome the *curse of dimensionality* (see [23] or [24], as examples using sparse grids with recombination technique for solving high-dimensional PDEs for derivatives pricing). Therefore, alternative formulations in terms of expectations are obtained in the next section, so that appropriate numerical Monte Carlo techniques could be efficiently applied.

2.4. Formulation in terms of expectations

In order to compute the total value adjustment when more than two stochastic factors are involved, a first approach could be made by using the Monte Carlo method, which is suitable to approximate expectations in a multidimensional framework, thus allowing to deal with problems that involve more than two stochastic factors.

First, in order to compute the values of U by using the Monte Carlo method in the nonlinear model (21), we apply the nonlinear Feynman–Kac theorem, that relates the solution of nonlinear PDEs with the solution of backward stochastic differential equations (BSDEs). The statement of the nonlinear Feynman–Kac theorem dates back from the seminal paper [25]. As the nonlinear term in (21) appears in the unknown U and not in the first order derivatives, Theorem 1.1 in the recent work by Beck et al. [26] can be applied to formulate the nonlinear problem (21) in terms of a nonlinear integral equation. Note that in [26] a large number of previous references on the nonlinear Feynman–Kac theorem are indicated, probably the here treated nonlinear PDE could be framed in many of them. Secondly, the linear Feynman–Kac theorem (see [22], for example) can be applied to the linear problem (22).

- If $M^D = V^D$, the total value adjustment at time t satisfies the equation

$$U(t,S_t,h_t) = E_t^{Q^D}\left[-\int_t^T e^{-f^D(u-t)}\Big(h_u\left(W^D(u,S_u) + U(u,S_u,h_u) - C^D(u)\right)^+ + \left(r^D + b^{D,C_0} - f^D\right)C^D(u)\Big)du\right]. \tag{23}$$

Note that (23) is an integral equation as the unknown U appears also at the right hand side in the integral. We are interested in the XVA at the current time $t = 0$, when the derivative is priced, that is to say

$$U(0,S_0,h_0) = E_0^{Q^D}\left[-\int_0^T e^{-f^D u}\Big(h_u\left(W^D(u,S_u) + U(u,S_u,h_u) - C^D(u)\right)^+ + \left(r^D + b^{D,C_0} - f^D\right)C^D(u)\Big)du\right]. \tag{24}$$

- If $M^D = W^D$, the total value adjustment at time t is given by

$$U(t,S_t,h_t) = E_t^{Q^D}\left[-\int_t^T \exp\left(-\int_t^u\left(\frac{h_r}{1-R_C}+f^D\right)dr\right)\left(h_u\left(W^D(u,S_u)-C^D(u)\right)^+ + \left(r^D + b^{D,C_0} - f^D\right)C^D(u)\right)du\right]. \tag{25}$$

Note that (25) gives an explicit formula for XVA. In particular, at time $t = 0$ we have

$$U(0,S_0,h_0) = E_0^{Q^D}\left[-\int_0^T \exp\left(-\int_0^u\left(\frac{h_r}{1-R_C}+f^D\right)dr\right)\left(h_u\left(W^D(u,S_u)-C^D(u)\right)^+ + \left(r^D + b^{D,C_0} - f^D\right)C^D(u)\right)du\right]. \tag{26}$$

3. Numerical methods

In the previous section, two problems for pricing the XVA have been posed, either in the event that $M^D = W^D$ (linear case) or in the event that $M^D = V^D$ (nonlinear case). In this section, we propose different numerical methods to compute the total value adjustment in both cases.

3.1. A Lagrange-Galerkin method

Problems governed by PDEs can be numerically solved by classical finite difference [27] or finite element methods [28] when the number of spatial-like variables is less or equal to three. Otherwise, these deterministic numerical methods based on geometrical discretizations become highly computational demanding to solve the problems and we have to make use of alternative methodologies.

In this section we will consider the solution of PDEs problems for obtaining the XVA where only two spatial-like variables are involved. We will compare the results obtained with the proposed methods to solve these PDEs problems with alternative techniques we propose for the case of a higher number of stochastic factors. Therefore, we first assume that the derivative is written on two underlying assets and the credit spread is a time dependent deterministic function. Moreover, we build this deterministic function as an approximation of the case with stochastic credit spread. Indeed it results to be a particular limit of the corresponding stochastic models.

Thus, we set $\sigma^h = 0$ both in the case of the exponential Vasicek dynamics (3) and of the CIR dynamics (4). In the first case, the credit spread is the solution of the following deterministic Initial Value Problem (IVP)

$$\begin{cases} dh(t) = \alpha h(t)\left(\theta - \log\left(h(t)\right)\right)dt, \\ h(0) = h_0, \end{cases}$$

so that

$$h(t) = \exp\left(\theta - e^{-\alpha t + \log\left(\theta - \log(h_0)\right)}\right). \tag{27}$$

In the case of CIR dynamics, the deterministic credit spread h is the solution of the following IVP

$$\begin{cases} dh(t) = \alpha h(t)\left(\theta - h(t)\right)dt, \\ h(0) = h_0, \end{cases}$$

so that

$$h(t) = \theta - \left(\theta - h_0\right)e^{\alpha t}. \tag{28}$$

In this framework, we propose a semi-Lagrangian time discretization technique combined with a finite element method for the spatial-like variables. This combination is usually referred to as Lagrange-Galerkin (LG) technique. For example, the semi-Lagrangian technique (also known as the method of characteristics) has been introduced in [29] for Navier–Stokes and transport equations and already used in [30] in combination with finite differences for option pricing. Recently, also in the context of the numerical solution of XVA models and combined with finite element method, i.e., Lagrange-Galerkin method, it has been used in [8,31].

As most of the numerical methods, this discretization technique needs the truncation of the initial unbounded spatial domain to a bounded one and the imposition of appropriate boundary conditions at certain boundaries of the bounded domain.

First, in order to pose more classical in terms of initial value problems instead of final value problems, we introduce the time-to-maturity, $\tau = T - t$. In this way, the problem (19) satisfied by the risk-free derivative can be written as

$$\begin{cases} \partial_\tau W^D - \mathcal{L}_S W^D + f^D W^D = 0, \\ W^D(0,S) = G(S). \end{cases} \tag{29}$$

Moreover, the nonlinear XVA problem (21) can be written as the following initial value problem:

$$\begin{cases} \partial_\tau U - \mathcal{L}_S U + f^D U = -h\left(W^D + U - C^D\right)^+ - \left(r^D + b^{D,C_0} - f^D\right) C^D, \\ U(0, S^1, S^2) = 0, \end{cases} \tag{30}$$

whereas the linear problem (22) is given by

$$\begin{cases} \partial_\tau U - \mathcal{L}_S U + \left(\dfrac{h}{1-R_C} + f^D\right) U = -h\left(W^D - C^D\right)^+ - \left(r^D + b^{D,C_0} - f^D\right) C^D, \\ U(0, S^1, S^2) = 0, \end{cases} \tag{31}$$

where $\tau \in (0, T)$ and $(S^1, S^2) \in \Omega = (0, S^1_\infty) \times (0, S^2_\infty)$.

Moreover, S^1_∞ and S^2_∞ are large enough numbers so that the value at the financial region of interest is not affected by the choice of the boundary conditions on the boundaries of the truncated domain Ω. Typically, this truncation argument is used in most PDEs models arising in financial problems.

Taking into account that the problem (29) for the risk free derivative price, the nonlinear problem (30) for the XVA and the linear problem (31) for the XVA involve the same differential operator $\mathcal{L}_S$, the partial differential equations of the three problems can be equivalently written as:

$$\partial_\tau W^D - \operatorname{div}(A \nabla W^D) + \mathbf{b} \cdot \nabla W^D + f^D W^D = 0, \tag{32}$$

$$\partial_\tau U^D - \operatorname{div}(A \nabla U^D) + \mathbf{b} \cdot \nabla U^D + f^D U = g_1(U^D, W^D), \tag{33}$$

$$\partial_\tau U^D - \operatorname{div}(A \nabla U^D) + \mathbf{b} \cdot \nabla U^D + \left(\frac{h}{1-R_C} + f^D\right) U = g_2(W^D), \tag{34}$$

respectively, where the matrix A and the vector $\mathbf{b}$ are given by

$$A = \frac{1}{2}\begin{pmatrix} (\sigma^{S^1})^2 (S^1)^2 & \sigma^{S^1}\sigma^{S^2}\rho^{S^1S^2} S^1 S^2 \\ \sigma^{S^1}\sigma^{S^2}\rho^{S^1S^2} S^1 S^2 & (\sigma^{S^2})^2 (S^2)^2 \end{pmatrix},$$
$$\mathbf{b} = \begin{pmatrix} \left((\sigma^{S^1})^2 + \frac{1}{2}\sigma^{S^1}\sigma^{S^2}\rho^{S^1S^2} - r^1 + q^1\right) S^1 \\ \left((\sigma^{S^2})^2 + \frac{1}{2}\sigma^{S^1}\sigma^{S^2}\rho^{S^1S^2} - r^2 + q^2\right) S^2 \end{pmatrix}, \tag{35}$$

while g_1 and g_2 denote the right hand side term of the nonlinear and the linear problems for the XVA, respectively.

In the following, we will focus on the linear risky problem, since the risk-free and nonlinear risky problems can be treated in a similar way. We will also omit the superscript D in the variables, as all of them are always written in the domestic currency.

Time discretization with semi-Lagrangian method

For the time discretization we use the semi-Lagrangian method. For this purpose, we introduce the material derivative of U given by

$$\frac{DU}{D\tau} = \frac{\partial U}{\partial \tau} + \mathbf{b} \cdot \nabla U = \frac{\partial U}{\partial \tau} + b_1 \frac{\partial U}{\partial S^1} + b_2 \frac{\partial U}{\partial S^2},$$

which represents the derivative along the characteristic curves associated to the vector field $\mathbf{b}$. In terms of the material derivative, the XVA linear equation in (34) turns into

$$\frac{DU}{D\tau} - \operatorname{div}(A \nabla U) + \left(\frac{h}{1-R_C} + f^D\right) U = g_2(W^D). \tag{36}$$

For the time discretization we consider a uniform mesh with a constant time step, $\Delta\tau = T/N_T > 0$, and the time mesh points $\tau^n = n\Delta\tau$, for $n = 0, 1, \ldots, N_T$, with $N_T > 1$ being a natural number, so that we have $N_T + 1$ time mesh points in the time interval $[0, T]$.

At each time mesh point τ^{n+1}, we approximate the material derivative by the upwinded finite differences scheme along the characteristics:

$$\frac{DU}{D\tau}(\tau^{n+1}, .) \approx \frac{U^{n+1} - U^n \circ \chi^n}{\Delta\tau}, \tag{37}$$

where $\chi^n(S^1, S^2) = \chi((S^1, S^2), \tau^{n+1}; \tau_n)$, with χ being the solution of the ODE problem associated to the characteristic curve:

$$\begin{cases} \dfrac{d\chi_1}{d\tau} = b_1(\chi_1) = \left((\sigma^{S^1})^2 + \frac{1}{2}\sigma^{S^1}\sigma^{S^2}\rho^{S^1S^2} - r^1 + q^1\right)\chi_1, \\ \chi_1(\tau^{n+1}) = S^1, \end{cases}$$

$$\begin{cases} \dfrac{d\chi_2}{d\tau} = b_2(\chi_2) = \left((\sigma^{S^2})^2 + \frac{1}{2}\sigma^{S^1}\sigma^{S^2}\rho^{S^1S^2} - r^2 + q^2\right)\chi_2, \\ \chi_2(\tau^{n+1}) = S^2. \end{cases}$$

Note that $\chi(\tau) = \chi((S^1, S^2), \tau^{n+1}; \tau)$ represents the characteristic curve associated to the velocity field $\mathbf{b}$ passing through (S^1, S^2) at instant τ^{n+1}.

In the method of characteristics (also known as semi-Lagrangian method) that we propose for the time discretization, we approximate the material derivative by expression (37) and replace it in (36) to pose the semi-discretized in time problem:

$$\begin{cases} \dfrac{U^{n+1} - U^n \circ \chi^n}{\Delta\tau} - \operatorname{div}(A\nabla U^{n+1}) + \left(\dfrac{h}{1-R_C} + f^D\right) U^{n+1} = g_2(W^{n+1}) \\ U^0(S^1, S^2) = 0\,, \end{cases}$$

where $U^n \approx U(\tau^n, \cdot)$. It is easy to check that the components of χ^n are given by:

$$\chi_1^n = S^1 \exp\left(-\left((\sigma^{S^1})^2 + \frac{1}{2}\sigma^{S^1}\sigma^{S^2}\rho^{S^1S^2} - r^1 + q^1\right)\Delta\tau\right),$$
$$\chi_2^n = S^2 \exp\left(-\left((\sigma^{S^2})^2 + \frac{1}{2}\sigma^{S^1}\sigma^{S^2}\rho^{S^1S^2} - r^2 + q^2\right)\Delta\tau\right).$$

Analysis of boundary conditions

In order to apply the finite element method to approximate the XVA, we need to truncate the unbounded domain and we consider the bounded domain $\Omega^* = (0,T)\times(0, S^1_\infty)\times(0, S^2_\infty)$. We follow Fichera's theory [32,33] to determine which boundaries of the domain need an imposed condition.

Let us introduce the notation $(x_0, x_1, x_2) = (\tau, S^1, S^2) \in \Omega^* = (0,T)\times(0, S^1_\infty)\times(0, S^2_\infty)$, and

$$\Gamma_i^{*,-} = \left\{(x_0, x_1, x_2) \in \partial\Omega^* \,/\, x_i = 0\right\}, \quad \Gamma_i^{*,+} = \left\{(x_0, x_1, x_2) \in \partial\Omega^* \,/\, x_i = x_i^\infty\right\}, i = 0, 1, 2.$$

Next, we define the matrix function A^* and the vector function $\mathbf{b}^*$ as

$$A^* = \frac{1}{2}\begin{pmatrix} 0 & 0 & 0 \\ 0 & (\sigma^{S^1})^2 x_1^2 & \rho^{S^1S^2}\sigma^{S^1}\sigma^{S^2}x_1x_2 \\ 0 & \rho^{S^1S^2}\sigma^{S^1}\sigma^{S^2}x_1x_2 & (\sigma^{S^2})^2 x_2^2 \end{pmatrix}, \qquad \mathbf{b}^* = \begin{pmatrix} -1 \\ (r^1 - q^1)x_1 \\ (r^2 - q^2)x_2 \end{pmatrix},$$

and the scalar function $c^* = -f^D$, so that Eq. (31) can be written as:

$$\sum_{i,j=0}^{2} a_{ij}^* \frac{\partial^2 U}{\partial x_i \partial x_j} + \sum_{i=0}^{2} b_i^* \frac{\partial U}{\partial x_i} + c^* U = 0\,.$$

Following [33], we deduce that we need to impose boundary conditions on $\Gamma_1^{*,+}$ ($S^1 = S^1_\infty$) and $\Gamma_2^{*,+}$ ($S^2 = S^2_\infty$) boundaries of Ω^* (see the Appendix for the details). Analogously to the boundaries of Ω^*, we introduce the notation for the boundaries of the spatial-like domain Ω as follows:

$$\Gamma_i^- = \left\{(S^1, S^2) \in \partial\Omega \,/\, S^i = 0\right\}, \quad \Gamma_i^+ = \left\{(S^1, S^2) \in \partial\Omega \,/\, S^i = S^i_\infty\right\}, i = 0, 1, 2.$$

In view of the previous arguments, we just need to impose boundary conditions on Γ_1^+ and Γ_2^+ for the PDEs formulations posed in the domain Ω.

Proposed boundary conditions on Γ_1^+ ($S^1 = S^1_\infty$). In order to deduce the conditions to impose on the right boundary of the domain, we make use of a previous methodology [8,34,35]. We consider Eq. (31), divide by $(S^1)^2$ and make S^1 tend to infinity, thus obtaining

$$\frac{1}{2}(\sigma^{S^1})^2 \frac{\partial^2 U}{\partial (S^1)^2} = 0\,,$$

so that we can write U as:

$$U(\tau, S^1, S^2) = H_0(\tau) + H_1(\tau)S^1 + H_2(\tau)S^2 + H_3(\tau)S^1S^2 + H_4(\tau)(S^2)^2\,.$$

Eq. (31) can be written, in this particular case, as

$$\partial_\tau U - \operatorname{div}(\widehat{A}\nabla U) + \widehat{\mathbf{b}}\cdot\nabla U + \left(\frac{h}{1-R_C} + f^D\right) U = g_2(W),$$

where

$$\widehat{A} = \frac{1}{2}\begin{pmatrix} 0 & \sigma^{S^1}\sigma^{S^2}\rho^{S^1S^2}S^1S^2 \\ \sigma^{S^1}\sigma^{S^2}\rho^{S^1S^2}S^1S^2 & (\sigma^{S^2})^2(S^2)^2 \end{pmatrix},$$

and the time discretization by the characteristics method leads to

$$U^{n+1} - \Delta\tau \operatorname{div}(\widehat{A}\nabla U^{n+1}) + \left(\frac{h}{1-R_C} + f^D\right)\Delta\tau\, U^{n+1} = \Delta\tau\, g_2(W^{n+1}) + U^n \circ \widehat{\chi}^n,$$

where $\widehat{\chi}^n$ (related to the velocity field $\widehat{\mathbf{b}}$) is given by

$$\begin{cases} \widehat{\chi}_1^n(S^1, S^2) = S^1 \exp\left(-\left(\frac{1}{2}\sigma^{S^1}\sigma^{S^2}\rho^{S^1S^2} - r^1 + q^1\right)\Delta\tau\right), \\ \widehat{\chi}_2^n(S^1, S^2) = S^2 \exp\left(-\left((\sigma^{S^2})^2 + \frac{1}{2}\sigma^{S^1}\sigma^{S^2}\rho^{S^1S^2} - r^2 + q^2\right)\Delta\tau\right). \end{cases}$$

Thus,

$$\left(1+\left(\frac{h}{1-R_C}+f^D\right)\Delta\tau\right)U^{n+1}-\Delta\tau\,\mathrm{div}\,(\widehat{A}\nabla U^{n+1})=\Delta\tau\,g_2(W^{n+1})+U^n\circ\widehat{\chi}^n$$

or, equivalently,

$$\begin{aligned}&\left(1+\left(\frac{h}{1-R_C}+f^D\right)\Delta\tau\right)\left[H_0(\tau)+H_1(\tau)S^1+H_2(\tau)S^2+H_3(\tau)S^1S^2+H_4(\tau)(S^2)^2\right]\\&\quad-\frac{\Delta\tau}{2}\frac{\partial}{\partial S^1}\left[0+\sigma^{S^1}\sigma^{S^2}\rho^{S^1S^2}S^1S^2\Big(H_2(\tau)+H_3(\tau)S^1+2H_4(\tau)S^2\Big)\right]\\&\quad-\frac{\Delta\tau}{2}\frac{\partial}{\partial S^2}\left[\sigma^{S^1}\sigma^{S^2}\rho^{S^1S^2}S^1S^2\Big(H_1(\tau)+H_3(\tau)S^2\Big)\right.\\&\quad\left.+(\sigma^{S^2})^2(S^2)^2\left(H_2(\tau)+H_3(\tau)S^1+2H_4(\tau)S^2\right)\right]\\&\quad=\Delta\tau\,g_2(W^{n+1})+U^n\circ\widehat{\chi}^n\,.\end{aligned}$$

If we choose $H_1(\tau)=H_2(\tau)=H_3(\tau)=H_4(\tau)=0$, then

$$U^{n+1}(S^1_\infty,S^2)=H_0^{n+1}=\frac{\Delta\tau\,g_2(W^{n+1})+U^n\circ\widehat{\chi}^n}{1+\left(\frac{h}{1-R_C}+f^D\right)\Delta\tau}\,.$$

Thus, a non homogeneous Dirichlet boundary condition is derived on the right boundary of the truncated domain.

In the risk-free problem, the Dirichlet boundary condition is given by:

$$U^{n+1}(S^1_\infty,S^2)=\frac{U^n\circ\widehat{\chi}^n}{1+f^D\Delta\tau}\,,$$

while the analogous condition in the nonlinear risky problem is

$$U^{n+1}(S^1_\infty,S^2)=\frac{\Delta\tau\,g_1(U^n,W^{n+1})+U^n\circ\widehat{\chi}^n}{1+f^D\Delta\tau}\,.$$

Proposed boundary conditions on Γ_2^+ ($S^2=S^2_\infty$). Similarly to what we did in the previous paragraph, on the upper boundary we can deduce an analogous Dirichlet boundary condition:

$$U^{n+1}(S^1,S^2_\infty)=\widetilde{H_0}^{n+1}=\frac{\Delta\tau\,g_2(W^{n+1})+U^n\circ\widetilde{\xi}^n}{1+\left(\frac{h}{1-R_C}+f^D\right)\Delta\tau}\,,$$

where $\widetilde{\xi}^n$ is given by:

$$\begin{cases}\widetilde{\xi}^n_1(S^1,S^2)=S^1\exp\left(-\left((\sigma^{S^1})^2+\frac{1}{2}\sigma^{S^1}\sigma^{S^2}\rho^{S^1S^2}-r^1+q^1\right)\Delta\tau\right)\\ \widetilde{\xi}^n_2(S^1,S^2)=S^2\exp\left(-\left(\frac{1}{2}\sigma^{S^1}\sigma^{S^2}\rho^{S^1S^2}-r^2+q^2\right)\Delta\tau\right)\,.\end{cases}$$

In the risk-free problem, the Dirichlet boundary condition is

$$U^{n+1}(S^1,S^2_\infty)=\frac{U^n\circ\widetilde{\xi}^n}{1+f^D\Delta\tau}\,,$$

while in the nonlinear problem it is given by

$$U^{n+1}(S^1,S^2_\infty)=\frac{\Delta\tau\,g_1(U^n,W^{n+1})+U^n\circ\widetilde{\xi}^n}{1+f^D\Delta\tau}\,.$$

Finite element method

As we propose to use a finite element method for the discretization in space, we first pose the variational formulation for the time discretized problem. At each time step, τ^n, we can use Green's formula and pose the variational formulation corresponding to the risky linear problem:

Find $U^{n+1}\in\left\{\varphi\in H^1(\Omega)/\varphi=H_5^{n+1}\text{ on }\Gamma_1^+,\varphi=\widetilde{H_5}^{n+1}\text{ on }\Gamma_2^+\right\}$ such that

$$\begin{aligned}&\int_\Omega U^{n+1}\varphi\,dS^1\,dS^2+\Delta\tau\int_\Omega A\nabla U^{n+1}\nabla\varphi\,dS^1\,dS^2+\Delta\tau\left(\frac{h(T-\tau^{n+1})}{1-R_C}+f^D\right)\int_\Omega U^{n+1}\varphi\,dS^1\,dS^2\\&\qquad=\int_\Omega(U^n\circ\chi^n)\varphi\,dS^1\,dS^2+\Delta\tau\int_\Omega g_2(W^{n+1})\varphi\,dS^1\,dS^2\,,\qquad\forall\varphi\in H^1_*(\Omega)\,,\end{aligned}$$

where $H^1_*(\Omega)=\left\{\varphi\in H^1(\Omega)\,/\,\varphi=0\text{ on }\Gamma_1^+\cup\Gamma_2^-\right\}$ and $H^1(\Omega)$ is a classical Sobolev space in the weak formulations of PDEs.

Next, we consider a triangular mesh of the domain and the finite element space of piecewise linear Lagrange polynomials [28]. More precisely, for fixed natural numbers $M > 0$ and $L > 0$, we consider a uniform triangulation, $\mathcal{T}$, of the computational domain Ω, the nodes of which are (S_i^1, S_j^2), with:

$$S_i^1 = i\Delta S^1\,(i = 0, 1, \dots, M+1), \qquad \Delta S^1 = \frac{S_\infty^1}{M+1},$$
$$S_j^2 = j\Delta S^2\,(j = 0, 1, \dots, L+1), \qquad \Delta S^2 = \frac{S_\infty^2}{L+1}.$$

Let us remark that a non uniform mesh can also be considered. We introduce the finite element spaces

$$Y_h = \left\{\varphi_h \in C(\Omega) \,/\, \varphi_h|_{T_k} \in \mathcal{P}_1, \forall T_k \in \mathcal{T}\right\}$$
$$Y_h^* = \left\{\varphi_h \in Y_h \,/\, \varphi_h = 0 \text{ on } \Gamma_1 \cup \Gamma_2\right\}$$

where T_k denotes a triangular element of the mesh for $k = 1, \dots, K$, the index h denotes a characteristic mesh size and $\mathcal{P}_1$ is the space of polynomials of degree less or equal than one. Then, we search U_h^{n+1} satisfying the boundary conditions and such that

$$\int_\Omega U_h^{n+1}\varphi_h\,dS^1\,dS^2 + \Delta\tau\int_\Omega A\nabla U_h^{n+1}\nabla\varphi_h\,dS^1\,dS^2 + \Delta\tau\left(\frac{h(T-\tau^{n+1})}{1-R_C} + f^D\right)\int_\Omega U_h^{n+1}\varphi_h\,dS^1\,dS^2$$
$$= \int_\Omega (U_h^n\circ\chi^n)\varphi\,dS^1\,dS^2 + \Delta\tau\int_\Omega g_2(U_h^n)\varphi_h\,dS^1\,dS^2, \qquad \forall\varphi_h \in Y_h^*. \tag{38}$$

The different integrals in (38) are approximated by adequate quadrature formulae, and the system of linear equations is solved by the LU method.

The risk-free problem is solved in a similar way; the differences with respect to the described risky linear problem concern the right hand side member and the coefficient of the unknown, W, in the PDE. Thus, the risk-free price is the solution of the following variational problem:

Find W_h^{n+1} such that:

$$\left(1 + \Delta\tau\, f^D\right)\int_\Omega W_h^{n+1}\varphi_h\,dS^1\,dS^2 + \Delta\tau\int_\Omega A\nabla W_h^{n+1}\nabla\varphi_h\,dS^1\,dS^2 = \int_\Omega (W_h^n\circ\chi^n)\varphi\,dS^1\,dS^2, \qquad \forall\varphi_h \in Y_h^*.$$

Fixed point iteration

In the nonlinear problem (30), an additional fixed point iteration method is implemented to approximate the solution. At each time step, τ^{n+1}, the scheme can be simply described, in terms of the strong formulation, as:

Let $U^{n+1,0} = U^n$, $\ell = 0$

For $\ell = 0, 1, \dots$

Solve $U^{n+1,\ell+1} - \Delta\tau\,\mathrm{div}\,(A\nabla U^{n+1,\ell+1}) + f^D\Delta\tau\,U^{n+1,\ell+1} = \Delta\tau\,g_1(U^{n+1,\ell}, W^{n+1}) + U^n\circ\chi^n$

until convergence: $\|U^{n+1,\ell+1} - U^{n+1,\ell}\|/\|U^{n+1,\ell+1}\| < \varepsilon$.

3.2. A Monte Carlo strategy

In the numerical examples in Section 4 we assume constant FX rates. We need a time discretization in order to discretize the dynamics of the underlying assets S^i $(i = 1, \dots, N)$ and of the credit spread h by using Euler–Maruyama scheme [36]. Thus, we choose a uniform mesh with Z nodes $0 = t_0 < t_1 < \cdots < t_{Z-1} = T$, and we denote by $\Delta t = t_z - t_{z-1}$ the distance between two consecutive nodes. Hence, we denote by $S_z^i = S^i(t_z)$, $\tilde{h}_z = \tilde{h}(t_z) = \log(h(t_z))$ and $h_z = h(t_z)$, and by $\Delta W_z^{S^i} = W_z^{S^i} - W_{z-1}^{S^i}$, for $i = 1, \dots, N$, and $\Delta W_z^h = W_z^h - W_{z-1}^h$ correlated Brownian increments to incorporate correlations between assets and between assets and credit spread. Therefore, for the underlying assets $S^1, \dots, S^N$ we have

$$S_{z+1}^i = S_z^i + (r^i - q^i)S_z^i\,\Delta t + \sigma^{S^i}S_z^i\,\Delta W_z^{S^i}$$

and for the credit spread with the exponential Vasicek dynamics we have

$$h_{z+1} = e^{\tilde{h}_{z+1}}, \quad \text{with} \quad \tilde{h}_{z+1} = \tilde{h}_z + \alpha(\theta - \tilde{h}_z)\Delta t + \sigma^h\Delta W_z^h.$$

In the case of the CIR model for the credit spread, the Euler–Maruyama scheme

$$h_{z+1} = h_z + \alpha(\theta - h_z)\Delta t + \sigma^h\sqrt{h_z}\Delta W_z^h$$

can lead to negative values since the Gaussian increment is not bounded from below, even if the Feller condition is satisfied and, thus, the continuous version of the process is positive. Therefore, we use the "full truncation" scheme proposed in [37], given by

$$h_{z+1} = h_z + \alpha(\theta - h_z^+)\Delta t + \sigma^h\sqrt{h_z^+}\Delta W_z^h.$$

The nonlinear case ($M = V^D$)

When $M = V^D$, a fixed-point method, or Picard iteration method, is implemented to compute the XVA price, given by the integral Eq. (24). Thus, we start from $U^0 = 0$ and recursively compute:

$$U^{\ell+1}(0,S,h) = E_0^{Q^D}\left[-\int_0^T e^{-f^D u}\Big(h_u\left(W^D(u,S_u)+U^\ell(u,S_u,h_u)-C^D(u)\right)^+ + \left(r^D+b^{D,C_0}-f^D\right)C^D(u)\Big)du \,\middle|\, S_0=S, h_0=h\right] \tag{39}$$

for $\ell = 0,1,2,\ldots$ until convergence is attained.

At each iteration (39) of the fixed-point algorithm of the nonlinear model the computation of an integral term is required. We consider either a simple rectangular or simple trapezoidal quadrature formula. Therefore, if we denote by $I^{NL,\ell}$ the integral in the right hand side of (39), thus

$$I^{NL,\ell} = \int_0^T e^{-f^D u}\Big(h_u\left(W^D(u,S_u)+U^\ell(u,S_u,h_u)-C^D(u)\right)^+ + \left(r^D+b^{D,C_0}-f^D\right)C^D(u)\Big)du,$$

then we approximate the integral as follows:

$$I^{NL,\ell} \simeq T\left[h_u\left(W^D(0,S_0)+U^\ell(0,S_0,h_0)-C^D(0)\right)^+ + \left(r^D+b^{D,C_0}-f^D\right)C^D(0)\right] \tag{40}$$

or

$$I^{NL,\ell} \simeq \frac{T}{2}\left[e^{-f^D T}\Big(h_T\left(W^D(T,S_T)-C^D(T)\right)^+ + \left(r^D+b^{D,C_0}-f^D\right)C^D(T)\Big) + \Big(h_0\left(W^D(0,S_0)+U^\ell(0,S_0,h_0)-C^D(0)\right)^+ + \left(r^D+b^{D,C_0}-f^D\right)C^D(0)\Big)\right]. \tag{41}$$

In the nonlinear case we use only simple quadrature formulas, because we just know the final value of U, that is $U_T = 0$, while composite formulas require to know the values of U at internal nodes of our time discretization. One could approximate the value of U at each node going backwards from the last node, although in this way a nested Monte Carlo problem arises. However, in order to improve our estimates we also implement the multilevel Picard iterations method proposed in [19,38], and recalled in Section 3.3, that allows to consider the values at the internal nodes of the time discretization.

The linear case ($M = W^D$)

When $M = W^D$, (26) gives an explicit expression for the XVA price that is computed with the help of numerical formulae for the approximation of the integral that use the time discretization stated above. As in the case of the nonlinear model, we use either a rectangular or a trapezoidal formula, but in the linear case also composite formulae can be implemented. Therefore, if we denote by I^L the integral in the right hand side of (26),

$$I^L = \int_0^T \exp\left(-\int_0^u\left(\frac{h_r}{1-R_C}+f^D\right)dr\right)\Big(h_u\left(W^D(u,S_u)-C^D(u)\right)^+ + \left(r^D+b^{D,C_0}-f^D\right)C^D(u)\Big)du, \tag{42}$$

then we approximate the integral either with a simple rectangular or a simple trapezoidal formula. Moreover, we approximate the integral (42) with the rectangular and the trapezoidal composite formulas given by

$$I^L \simeq \Delta t\sum_{z_1=0}^{Z-2}\exp\left(-\Delta t\sum_{z_2=0}^{z_1-1}\left(\frac{h_{t_{z_2}}}{1-R_C}+f\right)\right)\left(h_{z_1}\left(W^D(t_{z_1},S_{z_1})-C^D(t_{z_1})\right)^+ + \left(r^D+b^{D,C_0}-f^D\right)C^D(t_{z_1})\right)$$

and

$$I^L \simeq \frac{\Delta t}{2}\sum_{z_1=0}^{Z-2}\Bigg[\exp\left(-\frac{\Delta t}{2}\sum_{z_2=0}^{z_1-1}\left(\frac{h_{t_{z_2}}+h_{t_{z_2+1}}}{1-R_C}+2f^D\right)\right)\left(h_{z_1}\left(W^D(t_{z_1},S_{z_1})-C^D(t_{z_1})\right)^+ + \left(r^D+b^{D,C_0}-f^D\right)C^D(t_{z_1})\right) + \exp\left(-\frac{\Delta t}{2}\sum_{z_2=0}^{z_1}\left(\frac{h_{t_{z_2}}+h_{t_{z_2+1}}}{1-R_C}+2f^D\right)\right)\Big(h_{z_1+1}\left(W^D(t_{z_1+1},S_{z_1+1})-C^D(t_{z_1+1})\right)^+ + \left(r^D+b^{D,C_0}-f^D\right)C^D(t_{z_1+1})\Big)\Bigg]. \tag{43}$$

3.3. A multilevel Picard iteration scheme

In this subsection we briefly describe the main idea in the Multilevel Picard Iteration (MPI) method. For further details about the method, we address the reader to [19], for example.

The multilevel Picard iteration method is based in the adaptation of the multilevel Monte Carlo approach of Heinrich [39,40] and Giles [41] to the Picard approximation method. The multilevel Monte Carlo path simulations are based on the multigrid ideas, that facilitate the reduction of the computational complexity when estimating an expected value derived from a stochastic differential equation via Monte Carlo path simulations.

In order to apply the multilevel Picard iteration, we define function $\boldsymbol{\Phi}$ by

$$(\boldsymbol{\Phi}(\mathfrak{u}))(s,x) = \mathbb{E}_s^Q\left[-\int_s^T e^{-f^D(t-s)} \left(h_t\left(W^D(t,S_t) + \mathfrak{u} - C^D(t)\right)^+ + \left(r^D + b^{D,C_0} - f^D\right) C^D(t)\right) dt \,\middle|\, x = (S_s, h_s)\right]$$

and a sequence of Picard approximations $(\mathfrak{u}_n)_{n\in\mathbb{N}_0}$ such that $\mathfrak{u}_{n+1} = \boldsymbol{\Phi}(\mathfrak{u}_n)$ for all $n \in \mathbb{N}_0$. By using the Banach fixed-point theorem, it can be proved that the sequence $(\mathfrak{u}_n)_{n\in\mathbb{N}_0}$ converges at least exponentially fast to the solution of $u = \boldsymbol{\Phi}(u)$. Therefore, for all sufficiently large $n \in \mathbb{N}$, we have

$$\begin{aligned} u \approx \mathfrak{u}_n &= \mathfrak{u}_1 + \sum_{l=1}^{n-1}(\mathfrak{u}_{l+1} - \mathfrak{u}_l) = \boldsymbol{\Phi}(\mathfrak{u}_0) + \sum_{l=1}^{n-1}(\boldsymbol{\Phi}(\mathfrak{u}_l) - \boldsymbol{\Phi}(\mathfrak{u}_{l-1})) \\ &\approx \Psi_{n,\rho}(\mathfrak{u}_0) + \sum_{l=1}^{n-1}(\Psi_{n-l,\rho}(\mathfrak{u}_l) - \Psi_{n-l,\rho}(\mathfrak{u}_{l-1})), \end{aligned} \tag{44}$$

where $\Psi_{n,\rho}(\mathfrak{u}_l)$ is a discrete approximation of $\boldsymbol{\Phi}(\mathfrak{u}_l)$ with $m_{n,l,\rho}$ Monte Carlo paths. More precisely,

$$\begin{aligned} \left(\Psi_{n,\rho}\left(\mathfrak{u}_l\right)\right)(s,x) = -\frac{1}{m_{n,l,\rho}} \sum_{i=1}^{m_{n,l,\rho}} \sum_{t\in]s,T]} q_s^{n,l,\rho}(t) \\ e^{-f^D(t-s)}\left(h_t^{i,n,x}\left(W^D(t,S_t^{i,n,x}) + \mathfrak{u}_l - C^D(t)\right)^+ + \left(r^D + b^{D,C_0} - f^D\right) C^D(t)\right), \end{aligned}$$

where $(q^{n,l,\rho})_{n,l,\rho\in\mathbb{N}_0, l<n}$ denotes the family of quadrature rules for the approximation of the integral and the superscripts i, n, x refer to the ith Monte Carlo path with initial point x in the nth Picard iteration. In particular, in our numerical examples we have chosen $m_{n,l,\rho} = \rho^{n-l}$, as also proposed in [19].

Note that the quadrature rules $q^{n,l,\rho}$ are just functions on $[0,T]$ which have non-zero values only on a finite subset of $[0,T]$. In our numerical examples, we have chosen the left-rectangle rule with ρ^{n-l} rectangles, so that, for $s \in]0,T]$,

$$q_s^{n,l,\rho} = \frac{T-s}{\rho^{n-l}}\,\mathbb{1}_{s+i\frac{T-s}{\rho^{n-l}},i\in\mathbb{N}_0}(t), \quad t \in]s,T].$$

Since the XVA price in (24) can be seen as solution of $\mathfrak{u} = \boldsymbol{\Phi}(\mathfrak{u})$, from (44) we obtain our multilevel Picard iteration scheme:

$$\begin{cases} U_{0,\rho} = u_0, \\ U_{n,\rho} = \Psi_{n,\rho}\left(U_{0,\rho}\right) + \sum_{l=1}^{n-1}\left(\Psi_{n-l,\rho}\left(U_{l,\rho}\right) - \Psi_{n-l,\rho}\left(U_{l-1,\rho}\right)\right). \end{cases} \tag{45}$$

This recursive approximation scheme keeps the computational cost moderate compared to the desired approximation precision (see, for example, [19]).

Note that in the original multilevel Monte Carlo approach the different levels correspond to approximations with different step sizes in time or space, while in the multilevel Picard iterations method different levels correspond to different stages of the Picard iteration. Therefore, the approximations (45) are "full history recursive" in the sense that for every $n, \rho \in \mathbb{N}$ the "full history" of approximations, i.e., $U_{0,\rho}, U_{1,\rho}, \ldots, U_{n-1,\rho}$, needs to be computed recursively in order to compute $U_{n,\rho}$.

Relative approximation increments

In Section 4 the empirical convergence of the algorithm is tested. More precisely, we compute

$$U_{\rho,\rho}^i, \text{ for } (\rho,i) \in \{1,\ldots,\rho_{max}\} \times \{1,\ldots,N_{runs}\},$$

for fixed values of maximum ρ, ρ_{max}, and number of runs, N_{runs}. Then, we define the Relative Approximation Increments (RAI) of parameters ρ_{max} and N_{runs} as

$$RAI\left(\rho;\rho_{max},N_{runs}\right) = \frac{\frac{1}{N_{runs}}\sum_{i=1}^{10}\left|U_{\rho+1,\rho+1}^i - U_{\rho,\rho}^i\right|}{\frac{1}{N_{runs}}\sum_{i=1}^{10}\left|U_{\rho_{max},\rho_{max}}^i\right|}, \tag{46}$$

for $\rho = 1,\ldots,\rho_{max}-1$. The empirical convergence is shown by plotting the Relative Approximation Increments $RAI\left(\rho;\rho_{max},N_{runs}\right)$, for $\rho = 1,\ldots,\rho_{max}-1$, against ρ. In particular, in our numerical tests we have chosen $\rho_{max} = 5$ and $N_{runs} = 10$, as in one of the examples proposed in [19].

Table 1
Financial data.

$r = (0.05, 0.03)$	$f^D = 0.06$	$R_C = 0.30$
$q = (0.03, 0.02)$	$r^D = 0.04$	
$\sigma^S = (0.30, 0.20)$	$b^{D,C_0} = 0.01$	

Table 2
Counterparty's credit spread data. Values are in basis points (bps).

Exp Vasicek	$h_0 = 200$	$\alpha = 4.97$	$\theta = 3.83$	$\sigma^h = 1.41$
CIR	$h_0 = 200$	$\alpha = 1.29$	$\theta = 51.79$	$\sigma^h = 4.50$

4. Numerical results

In this section we report some tests that illustrate the behaviour of the previously described numerical methods when they are used for the evaluation of different multiasset options [42] in the presence of counterparty risk.

Our aim is to analyse how the choice of the mark-to-market, the initial values of the underlying assets and of the counterparty's credit spread, as well as its dynamics, affect the total valuation adjustment and, therefore, the price of the financial derivative.

In all examples we consider constant FX rates, so that we have dropped subindex t to use the notation X^{D,C_j} instead of X_t^{D,C_j} throughout this section.

The elapsed computational time depends on the number of the underlying assets and on the value assigned to the mark-to-market value M^D, as well as on the choice of the parameters associated to the numerical methods (such as, N_P, Z and those involved in the discretization of PDEs).

Unless otherwise stated, we have used data listed in Tables 1 and 2. We have denoted by $r = (r^1, r^2)$ the vector of the short-term rates in the foreign markets, $q = (q^1, q^2)$ the vector of the dividends paid by the corresponding underlying assets and $\sigma^S = (\sigma^{S^1}, \sigma^{S^2})$ the vector of the assets volatilities.

It is important to point out that the parameters for the dynamics of the credit spread are borrowed from [21], where the credit spread is calibrated on market data. So, they are calibrated parameters.

Moreover, the maturities of the options are set to $T = 1$ year. Finally, we have chosen the collateral account C^D to be a percentage $C^{\%} = 0.25$ of the risk-free derivative value.

Concerning the parameters of the numerical methods, for the Monte Carlo method we have used $N_P = 10^4$ paths and $Z = 252$ time nodes. Moreover, different quadrature formulae have been used to approximate the involved integrals; in particular, the abbreviations SimpR, SimpT, CompR and CompT are used in the following tables to denote the simple and composite rectangular and trapezoidal formulae. For the Lagrange-Galerkin method, different meshes have been used and the number of nodes in both directions and the number of time steps are indicated in the different tables containing the results. Moreover, for the fixed point iteration methods that has been additionally applied in the nonlinear PDEs, the tolerance of the stopping test in the relative error between two consecutive iterations has been set to 10^{-16}.

In the following, we present and analyse numerical results related to a *spread option*, an *exchange option* and a *sum of call options*. For each product, we first assume the counterparty credit spread is a time dependent deterministic function and the derivative is written on two stochastic underlying assets. In this case, we compare the Lagrange-Galerkin results with the Monte Carlo 99% confidence intervals. In the nonlinear case, we also show that the Multilevel Picard Iteration values are in agreement with the ones obtained with the Lagrange-Galerkin method. In a more general case, when the credit spread is stochastic and, eventually, the derivative depends on more than two stochastic underlying assets, we do not address the solution of the PDE formulation.

In all tables we use LG for the results obtained with the proposed Lagrange-Galerkin method for PDEs and MPI for the computed results with the Multilevel Picard Iteration method.

All tests corresponding to Monte Carlo and MPI methods have been performed by using Matlab on an Intel(R) Core(TM) i7-8550U, 1.99 GHz, 16 GB (RAM), x64-based processor. The tests corresponding to Lagrange-Galerkin method have been developed by using C++ on an AMD Ryzen7(R) 5700X, 64 GB (RAM) processor.

4.1. Spread option

We first assume the hedger buys from a counterparty a *spread option*, written on two underlying assets, each of them being denominated in a different currency. The payoff function is given by

$$G(t, S^1, S^2) = \left(X^{D,C_2} S^2 - X^{D,C_1} S^1 - K\right)^+,$$

where K is the strike value in the domestic currency D.

In our numerical tests, we have set the value of the strike to $K = 15$ and we have selected nodes that are in the proximity of the at-the-money line, i.e., $X^{D,C_2} S^2 - X^{D,C_1} S^1 - K = 0$.

Table 3
Spread option. Comparison of Monte Carlo and Lagrange-Galerkin methods. Risk-free value (Test 1).

Risk-free value			
$(S^{1,D}, S^{2,D})$	Monte Carlo	LG	
		$21 \times 21, 100$	$41 \times 41, 200$
$(9, 21)$	$[0.7784, 0.8782]$	0.7899	0.8122
$(9, 24)$	$[2.0457, 2.2119]$	2.0893	2.1063
$(9, 27)$	$[3.9481, 4.1775]$	4.0258	4.0434
$(15, 27)$	$[1.3606, 1.5105]$	1.4168	1.4214
$(15, 30)$	$[2.7155, 2.9316]$	2.8016	2.8041
$(15, 33)$	$[4.5435, 4.8233]$	4.6633	4.6678
$(21, 33)$	$[2.0091, 2.2111]$	2.0997	2.0933
$(21, 36)$	$[3.4188, 3.6868]$	3.5380	3.5302
$(21, 39)$	$[5.2017, 5.5334]$	5.3507	5.3440

Table 4
Spread option, nonlinear problem and deterministic exponential Vasicek credit spread. Comparison of Monte Carlo, multilevel Picard iteration and Lagrange-Galerkin methods. Total value adjustment (Test 1).

Total value adjustment						
$(S^{1,D}, S^{2,D})$	Monte Carlo		MPI		LG	
	SimpR	SimpT	$\rho = 4$	$\rho = 5$	$21 \times 21, 100$	$41 \times 41, 200$
$(9, 21)$	$[-0.0109, -0.0097]$	$[-0.0059, -0.0052]$	-0.0019	-0.0020	-0.0021	-0.0021
$(9, 24)$	$[-0.0274, -0.0253]$	$[-0.0148, -0.0137]$	-0.0049	-0.0053	-0.0054	-0.0053
$(9, 27)$	$[-0.0515, -0.0487]$	$[-0.0280, -0.0264]$	-0.0100	-0.0102	-0.0103	-0.0102
$(15, 27)$	$[-0.0188, -0.0169]$	$[-0.0102, -0.0091]$	-0.0035	-0.0036	-0.0037	-0.0036
$(15, 30)$	$[-0.0363, -0.0336]$	$[-0.0197, -0.0182]$	-0.0069	-0.0070	-0.0072	-0.0071
$(15, 33)$	$[-0.0595, -0.0560]$	$[-0.0323, -0.0304]$	-0.0113	-0.0117	-0.0120	-0.0118
$(21, 33)$	$[-0.0274, -0.0249]$	$[-0.0149, -0.0135]$	-0.0052	-0.0052	-0.0054	-0.0053
$(21, 36)$	$[-0.0456, -0.0423]$	$[-0.0247, -0.0229]$	-0.0087	-0.0088	-0.0091	-0.0090
$(21, 39)$	$[-0.0683, -0.0642]$	$[-0.0371, -0.0349]$	-0.0132	-0.0135	-0.0137	-0.0135

Table 5
Spread option, nonlinear problem and deterministic CIR credit spread. Comparison of Monte Carlo, multilevel Picard iteration and Lagrange-Galerkin methods. Total value adjustment (Test 1).

Total value adjustment						
$(S^{1,D}, S^{2,D})$	Monte Carlo		MPI		LG	
	SimpR	SimpT	$\rho = 4$	$\rho = 5$	$21 \times 21, 100$	$41 \times 41, 200$
$(9, 21)$	$[-0.0109, -0.0097]$	$[-0.0074, -0.0066]$	-0.0057	-0.0062	-0.0061	-0.0062
$(9, 24)$	$[-0.0274, -0.0253]$	$[-0.0186, -0.0172]$	-0.0152	-0.0161	-0.0160	-0.0160
$(9, 27)$	$[-0.0515, -0.0487]$	$[-0.0351, -0.0332]$	-0.0309	-0.0310	-0.0308	-0.0308
$(15, 27)$	$[-0.0188, -0.0169]$	$[-0.0127, -0.0115]$	-0.0107	-0.0108	-0.0109	-0.0108
$(15, 30)$	$[-0.0363, -0.0336]$	$[-0.0247, -0.0229]$	-0.0214	-0.0214	-0.0214	-0.0214
$(15, 33)$	$[-0.0595, -0.0560]$	$[-0.0406, -0.0382]$	-0.0346	-0.0356	-0.0356	-0.0355
$(21, 33)$	$[-0.0274, -0.0249]$	$[-0.0187, -0.0169]$	-0.0161	-0.0158	-0.0161	-0.0160
$(21, 36)$	$[-0.0456, -0.0423]$	$[-0.0311, -0.0288]$	-0.0268	-0.0269	-0.0271	-0.0269
$(21, 39)$	$[-0.0683, -0.0642]$	$[-0.0466, -0.0438]$	-0.0405	-0.0409	-0.0409	-0.0407

4.1.1. Test 1: Risk-free value.

We first compute the risk-free price of the spread option for different initial values of the underlying assets both with the Monte Carlo and the Lagrange-Galerkin methods. Note that the risk-free value obviously depends only on two stochastic factors, that are the two underlying assets, being independent of the credit spread.

Table 3 shows the computed risk-free prices. The table header indicates the used method and the number of nodes (in both directions) and the number of time steps in the Lagrange-Galerkin method. We use the notation $S^{i,D} = X^{D,C_i} S^i$, for $i = 1, 2$, so that we can display all the prices in the same currency D. For each considered initial point $(S^{1,D}, S^{2,D})$, the risk-free value computed with Lagrange-Galerkin falls inside the Monte Carlo 99% confidence intervals, also in the case of the coarsest mesh.

4.1.2. Test 2: Nonlinear problem, deterministic time dependent credit spread.

We now consider the deterministic exponential Vasicek (27) and CIR (28) dynamics for the credit spread and compute the total value adjustment in the nonlinear case, when the PDE formulation is given by (21) and the formulation in terms of expectation is reported in (24). Note that in the case of deterministic counterparty's credit spread, only two stochastic factors are considered when pricing a spread option.

Tables 4 and 5 show the computed total value adjustment. The tables headers indicate the used quadrature formulae in Monte Carlo simulations, the value of parameter ρ in the multilevel Picard iteration method, and the number of nodes and time steps

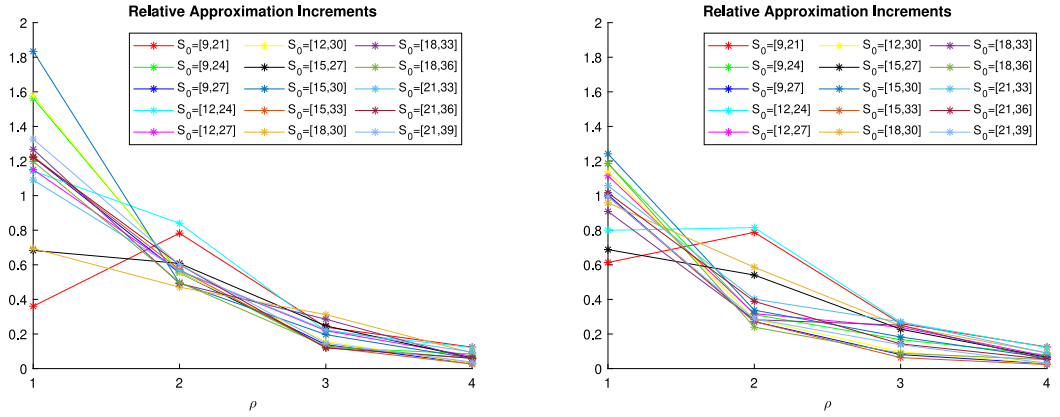

Fig. 3. Spread option with deterministic credit spread. Convergence of MPI with exponential Vasicek dynamics for credit spread on the left and CIR dynamics on the right (Test 2).

Table 6
Spread option, linear problem and deterministic exponential Vasicek credit spread. Comparison of Monte Carlo and Lagrange-Galerkin methods. Total value adjustment (Test 3).

Total value adjustment				
$(S^{1,D}, S^{2,D})$	Monte Carlo		LG	
	CompR	CompT	$21 \times 21, 100$	$41 \times 41, 200$
(9, 21)	[−0.0022, −0.0020]	[−0.0022, −0.0019]	−0.0021	−0.0021
(9, 24)	[−0.0055, −0.0051]	[−0.0055, −0.0051]	−0.0054	−0.0053
(9, 27)	[−0.0105, −0.0099]	[−0.0104, −0.0098]	−0.0103	−0.0102
(15, 27)	[−0.0038, −0.0034]	[−0.0038, −0.0034]	−0.0037	−0.0036
(15, 30)	[−0.0074, −0.0068]	[−0.0073, −0.0067]	−0.0072	−0.0071
(15, 33)	[−0.0121, −0.0114]	[−0.0120, −0.0113]	−0.0120	−0.0118
(21, 33)	[−0.0055, −0.0050]	[−0.0055, −0.0050]	−0.0054	−0.0053
(21, 36)	[−0.0092, −0.0086]	[−0.0092, −0.0085]	−0.0091	−0.0089
(21, 39)	[−0.0139, −0.0130]	[−0.0137, −0.0129]	−0.0137	−0.0135

in the Lagrange-Galerkin method. From both tables we can deduce that the multilevel Picard iteration and the Lagrange-Galerkin results are in agreement and they are closer to each other when setting $\rho = 5$ in the MPI method and taking a finer mesh in the LG one. However, MPI and LG values do not belong to the confidence intervals computed with Monte Carlo method, the results with trapezoidal formula being the closest ones to the MPI and LG results, especially in the case of CIR dynamics that are shown in Table 5.

The convergence of the multilevel Picard iteration method has been tested by computing the Relative Approximation Increments (RAI) defined in Section 3.3. We recall that in (46) we have set $\rho_{max} = 5$, $N_{runs} = 10$, and we have computed $RAI(\rho, \rho_{max}, N_{runs})$ for $\rho = 1, \ldots, 4$. Fig. 3 shows the empirical convergence of the method.

4.1.3. Test 3: Linear problem, deterministic time dependent credit spread.

Still considering the deterministic exponential Vasicek and CIR dynamics for the credit spread, we compute the XVA in the linear case, when the PDE formulation is given by (22) and the formulation in terms of expectation is reported in (26).

Tables 6 and 7 show the Monte Carlo confidence intervals computed with the composite rectangular and trapezoidal quadrature formulae and the Lagrange-Galerkin method values. The Monte Carlo confidence intervals coincide in the three or four decimal figures when using both composite formulae. We have also used simple quadrature formulae to deduce the confidence intervals, although we do not report these results, because they do not agree with the confidence intervals computed with the composite quadrature formulae and the XVA values computed with the Lagrange-Galerkin method. Instead, from Tables 6 and 7 we can see that the LG results belong to the reported Monte Carlo confidence intervals.

We also show in Table 8 the risky price of the spread option with an exponential Vasicek credit spread. Again, we can see that the results computed with the Lagrange-Galerkin method belong to the Monte Carlo 99% confidence intervals obtained with composite quadrature formulae.

4.1.4. Test 4: Nonlinear problem, stochastic credit spread.

We now consider the more general case when the credit spread is a stochastic process following either an exponential Vasicek (3) or a CIR (4) dynamics and the mark-to-market value is equal to the risky derivative value (nonlinear case). Note that in the case of stochastic credit spread of the counterparty, three stochastic factors are involved in the pricing of the spread option.

Table 7
Spread option, linear problem and deterministic CIR credit spread. Comparison of Monte Carlo and Lagrange-Galerkin methods. Total value adjustment (Test 3).

Total value adjustment				
$(S^{1,D}, S^{2,D})$	Monte Carlo		LG	
	CompR	CompT	$21 \times 21, 100$	$41 \times 41, 200$
$(9, 21)$	$[-0.0066, -0.0059]$	$[-0.0066, -0.0059]$	-0.0061	-0.0062
$(9, 24)$	$[-0.0167, -0.0155]$	$[-0.0167, -0.0154]$	-0.0160	-0.0160
$(9, 27)$	$[-0.0316, -0.0299]$	$[-0.0315, -0.0298]$	-0.0307	-0.0307
$(15, 27)$	$[-0.0114, -0.0103]$	$[-0.0114, -0.0103]$	-0.0109	-0.0108
$(15, 30)$	$[-0.0222, -0.0205]$	$[-0.0221, -0.0205]$	-0.0214	-0.0213
$(15, 33)$	$[-0.0365, -0.0344]$	$[-0.0364, -0.0343]$	-0.0355	-0.0354
$(21, 33)$	$[-0.0167, -0.0152]$	$[-0.0167, -0.0152]$	-0.0161	-0.0159
$(21, 36)$	$[-0.0279, -0.0259]$	$[-0.0278, -0.0258]$	-0.0270	-0.0268
$(21, 39)$	$[-0.0419, -0.0394]$	$[-0.0418, -0.0393]$	-0.0408	-0.0406

Table 8
Spread option, linear problem and deterministic exponential Vasicek credit spread. Comparison of Monte Carlo and Lagrange-Galerkin methods. Risky value (Test 3).

Risky value				
$(S^{1,D}, S^{2,D})$	Monte Carlo		LG	
	CompR	CompT	$21 \times 21, 100$	$41 \times 41, 200$
$(9, 21)$	$[0.7784, 0.8782]$	$[0.7784, 0.8782]$	0.7879	0.8101
$(9, 24)$	$[2.0457, 2.2119]$	$[2.0457, 2.2119]$	2.0839	2.1009
$(9, 27)$	$[3.9481, 4.1775]$	$[3.9481, 4.1775]$	4.0155	4.0332
$(15, 27)$	$[1.3606, 1.5105]$	$[1.3606, 1.5105]$	1.4132	1.4178
$(15, 30)$	$[2.7155, 2.9316]$	$[2.7155, 2.9316]$	2.7944	2.7970
$(15, 33)$	$[4.5435, 4.8233]$	$[4.5435, 4.8233]$	4.6514	4.6560
$(21, 33)$	$[2.0091, 2.2111]$	$[2.0091, 2.2111]$	2.0943	2.0880
$(21, 36)$	$[3.4188, 3.6868]$	$[3.4188, 3.6868]$	3.5289	3.5213
$(21, 39)$	$[5.2017, 5.5334]$	$[5.2017, 5.5334]$	5.3369	5.3304

Table 9
Spread option, nonlinear problem and stochastic exponential Vasicek credit spread. Comparison of Monte Carlo and multilevel Picard iteration methods. Total value adjustment (Test 4).

Total value adjustment				
$(S^{1,D}, S^{2,D})$	Monte Carlo		MPI	
	SimpR	SimpT	$\rho = 4$	$\rho = 5$
$(9, 21)$	$[-0.0109, -0.0097]$	$[-0.0058, -0.0051]$	-0.0018	-0.0019
$(9, 24)$	$[-0.0274, -0.0253]$	$[-0.0147, -0.0136]$	-0.0050	-0.0051
$(9, 27)$	$[-0.0515, -0.0487]$	$[-0.0279, -0.0263]$	-0.0105	-0.0104
$(15, 27)$	$[-0.0188, -0.0169]$	$[-0.0099, -0.0089]$	-0.0035	-0.0033
$(15, 30)$	$[-0.0363, -0.0336]$	$[-0.0194, -0.0180]$	-0.0066	-0.0067
$(15, 33)$	$[-0.0595, -0.0560]$	$[-0.0321, -0.0302]$	-0.0116	-0.0116
$(21, 33)$	$[-0.0274, -0.0249]$	$[-0.0145, -0.0132]$	-0.0046	-0.0048
$(21, 36)$	$[-0.0456, -0.0423]$	$[-0.0243, -0.0226]$	-0.0082	-0.0084
$(21, 39)$	$[-0.0683, -0.0642]$	$[-0.0367, -0.0345]$	-0.0131	-0.0132

Tables 9 and 10 illustrate the computed XVA for some fixed initial values of the underlying assets. For each fixed value of $S^{1,D}$ we analyse three different possibilities: out of the money option, at the money option and in the money option, respectively. When considering a stochastic credit spread, we do not address the solution of the XVA pricing PDE with Lagrange-Galerkin method and we take MPI values as reference values. Indeed, we have seen in the case of the deterministic time dependent credit spread that MPI and LG results are very close, but not inside the Monte Carlo confidence intervals. The multilevel Picard iteration method is tested either with $\rho = 4$ or with $\rho = 5$. Moreover, we have tested the convergence of the MPI method for all the initial underlying assets values considered in the tables by plotting the relative approximation increments in Fig. 4. As for the deterministic credit spread case, the Monte Carlo confidence intervals, obtained with a simple Picard iteration, do not contain the multilevel Picard iteration results. As expected, the total value adjustment is negative because, when buying the derivative, the hedger will ask the counterparty for a reduction in the price due to the possibility of the counterparty's default. Also, we can see that the total value adjustment becomes more negative when the option is in the money and less negative when it is out of the money, indeed in the former case the hedger would be worst affected by the counterparty's default, because the option is more valuable.

Fig. 5 shows the total value adjustment for different underlying assets initial values computed with the multilevel Picard iteration method. In particular, each point of the plot shows the average MPI value on $N_{runs} = 10$ runs with the parameter ρ fixed to 4. The choice of the ρ value is due to the fact that from Tables 9 and 10 we infer that results with $\rho = 4$ and $\rho = 5$ are very close to each

Table 10
Spread option, nonlinear problem and stochastic CIR credit spread. Comparison of Monte Carlo and multilevel Picard iteration methods. Total value adjustment (Test 4).

Total value adjustment				
$(S^{1,D}, S^{2,D})$	Monte Carlo		MPI	
	SimpR	SimpT	$\rho = 4$	$\rho = 5$
(9, 21)	[−0.0109, −0.0097]	[−0.0069, −0.0061]	−0.0055	−0.0055
(9, 24)	[−0.0274, −0.0253]	[−0.0175, −0.0162]	−0.0142	−0.0146
(9, 27)	[−0.0515, −0.0487]	[−0.0335, −0.0317]	−0.0291	−0.0290
(15, 27)	[−0.0188, −0.0169]	[−0.0118, −0.0106]	−0.0102	−0.0197
(15, 30)	[−0.0363, −0.0336]	[−0.0231, −0.0214]	−0.0192	−0.0193
(15, 33)	[−0.0595, −0.0560]	[−0.0384, −0.0362]	−0.0330	−0.0328
(21, 33)	[−0.0274, −0.0249]	[−0.0172, −0.0157]	−0.0137	−0.0141
(21, 36)	[−0.0456, −0.0423]	[−0.0290, −0.0269]	−0.0239	−0.0243
(21, 39)	[−0.0683, −0.0642]	[−0.0439, −0.0413]	−0.0374	−0.0377

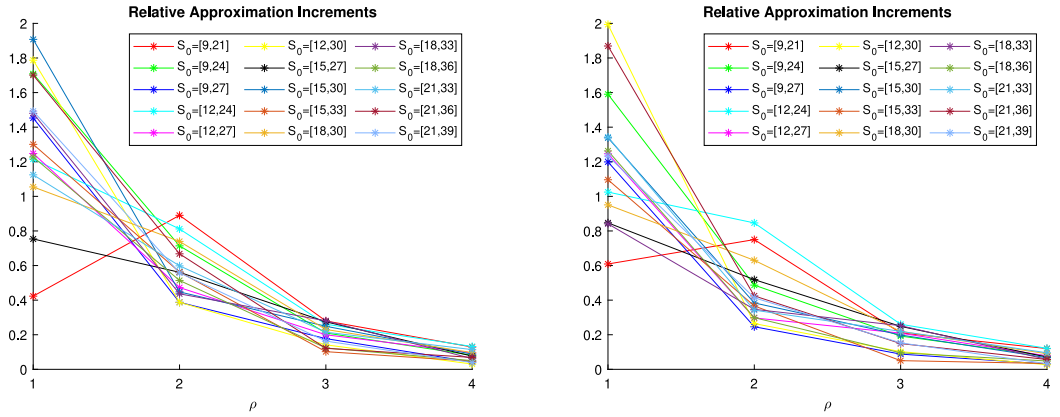

Fig. 4. Spread option with stochastic credit spread. Convergence of MPI with exponential Vasicek dynamics for credit spread on the left and CIR dynamics on the right (Test 4).

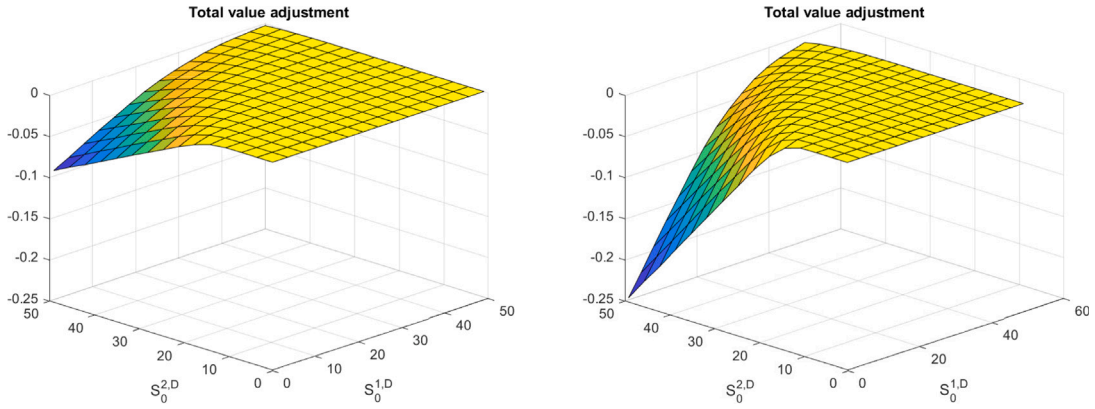

Fig. 5. Spread option in the nonlinear case. Total value adjustment with exponential Vasicek credit spread on the left and with CIR credit spread on the right (Test 4).

others and it is not worth to produce plots by using $\rho = 5$, that is more time consuming. In fact, one run of MPI with $\rho = 4$ takes slightly more than 1 s, but with $\rho = 5$ it takes about 340 s. From the figure it is evident that the XVA is more negative under the assumption of CIR credit spread than under the assumption of exponential Vasicek credit spread.

4.1.5. Test 5: Linear problem, stochastic credit spread.

We move to the linear problem with stochastic credit spread. Tables 11 and 12 show the Monte Carlo confidence intervals for the total value adjustment with exponential Vasicek and CIR credit spread, respectively. The confidence intervals coincide in the

Table 11
Spread option, linear problem and stochastic exponential Vasicek credit spread. Comparison of different quadrature formulae in Monte Carlo method. Total value adjustment (Test 5).

Total value adjustment				
$(S^{1,D}, S^{2,D})$	Monte Carlo			
	SimpR	SimpT	CompR	CompT
(9, 21)	[−0.0007, −0.0006]	[−0.0058, −0.0052]	[−0.0021, −0.0018]	[−0.0021, −0.0018]
(9, 24)	[−0.0020, −0.0017]	[−0.0148, −0.0137]	[−0.0055, −0.0050]	[−0.0054, −0.0050]
(9, 27)	[−0.0042, −0.0037]	[−0.0281, −0.0266]	[−0.0108, −0.0101]	[−0.0107, −0.0100]
(15, 27)	[−0.0012, −0.0010]	[−0.0100, −0.0090]	[−0.0036, −0.0032]	[−0.0035, −0.0031]
(15, 30)	[−0.0026, −0.0022]	[−0.0195, −0.0181]	[−0.0072, −0.0066]	[−0.0071, −0.0065]
(15, 33)	[−0.0046, −0.0040]	[−0.0323, −0.0305]	[−0.0122, −0.0114]	[−0.0120, −0.0113]
(21, 33)	[−0.0018, −0.0014]	[−0.0146, −0.0133]	[−0.0052, −0.0047]	[−0.0051, −0.0046]
(21, 36)	[−0.0032, −0.0027]	[−0.0246, −0.0228]	[−0.0089, −0.0082]	[−0.0088, −0.0082]
(21, 39)	[−0.0051, −0.0044]	[−0.0370, −0.0348]	[−0.0138, −0.0129]	[−0.0136, −0.0128]

Table 12
Spread option, linear problem and stochastic CIR credit spread. Comparison of different quadrature formulae in Monte Carlo method. Total value adjustment (Test 5).

Total value adjustment				
$(S^{1,D}, S^{2,D})$	Monte Carlo			
	SimpR	SimpT	CompR	CompT
(9, 21)	[−0.0029, −0.0025]	[−0.0069, −0.0061]	[−0.0060, −0.0053]	[−0.0060, −0.0053]
(9, 24)	[−0.0077, −0.0071]	[−0.0176, −0.0163]	[−0.0154, −0.0142]	[−0.0154, −0.0142]
(9, 27)	[−0.0153, −0.0144]	[−0.0337, −0.0318]	[−0.0296, −0.0280]	[−0.0296, −0.0279]
(15, 27)	[−0.0049, −0.0043]	[−0.0118, −0.0107]	[−0.0103, −0.0092]	[−0.0102, −0.0092]
(15, 30)	[−0.0100, −0.0092]	[−0.0233, −0.0216]	[−0.0203, −0.0188]	[−0.0202, −0.0187]
(15, 33)	[−0.0172, −0.0161]	[−0.0386, −0.0364]	[−0.0338, −0.0319]	[−0.0338, −0.0318]
(21, 33)	[−0.0071, −0.0064]	[−0.0173, −0.0158]	[−0.0150, −0.0136]	[−0.0150, −0.0136]
(21, 36)	[−0.0124, −0.0114]	[−0.0292, −0.0271]	[−0.0254, −0.0235]	[−0.0253, −0.0235]
(21, 39)	[−0.0194, −0.0181]	[−0.0442, −0.0415]	[−0.0386, −0.0363]	[−0.0385, −0.0362]

three or four decimal figures when using both composite formulae, that we take as reference values, while the simple formulae give results that are a bit far from the composite formulae results.

Fig. 6 shows the risky price and the total value adjustment. For each point of the plots we consider the average Monte Carlo value obtained by approximating the integral in the XVA formula with composite trapezoidal formula. As for the nonlinear case, the XVA is more negative when the credit spread is modelled as CIR process. However, the difference between the plotted risky prices under the two alternative assumptions for the dynamics of the credit spread is not evident, because the difference between the total value adjustments is negligible with respect to the derivative prices.

From Tables 11 and 12 and from Fig. 6 we can take out the same conclusions to those drawn in the nonlinear case: the XVA becomes more negative when the price of the asset S^2 increases, namely when the option is in the money and the XVA approaches to zero when the S^2 price decreases, namely when the option is out of the money.

4.2. Exchange option

In this subsection, we assume that the default-free hedger buys from the defaultable counterparty an *exchange option*, written on an underlying asset S^1, denominated in the domestic currency, and an underlying asset S^2, denominated in a foreign currency C_2. Hence, the payoff function of the option is given by

$$G(t, S^1, S^2) = (S^1 - X^{D,C_2} S^2)^+.$$

4.2.1. Test 6: Nonlinear problem, deterministic time dependent credit spread.

First, we compare the XVA computed with different numerical methods in the case of the nonlinear problem with a deterministic credit spread. Note that in the setting of deterministic credit spread of the counterparty, only two stochastic factors are involved in the pricing of exchange options.

The points where we show the different values are close to the at the money line, $S^1 - X^{D,C_2} S^2 = 0$.

Tables 13 and 14 show the results for the XVA. The multilevel Picard iteration and the Lagrange-Galerkin methods values are quite far from the Monte Carlo confidence intervals obtained with a fixed-point method and simple quadrature formulae for the approximation of the integral in the XVA expression in (24). The MPI and the LG results are closer to each other if we take $\rho = 5$ in the MPI method and a mesh of 41×41 nodes with 200 time steps in the LG method, except for the last two points when we assume an exponential Vasicek dynamics for the credit spread and in the last three points under the assumption of a CIR credit spread. This is due to the fact that the Lagrange-Galerkin results are not reliable near the fixed right and upper boundaries of the computational domain, in our case located at $S^1_\infty = 60$ and $S^2_\infty = 60$, respectively.

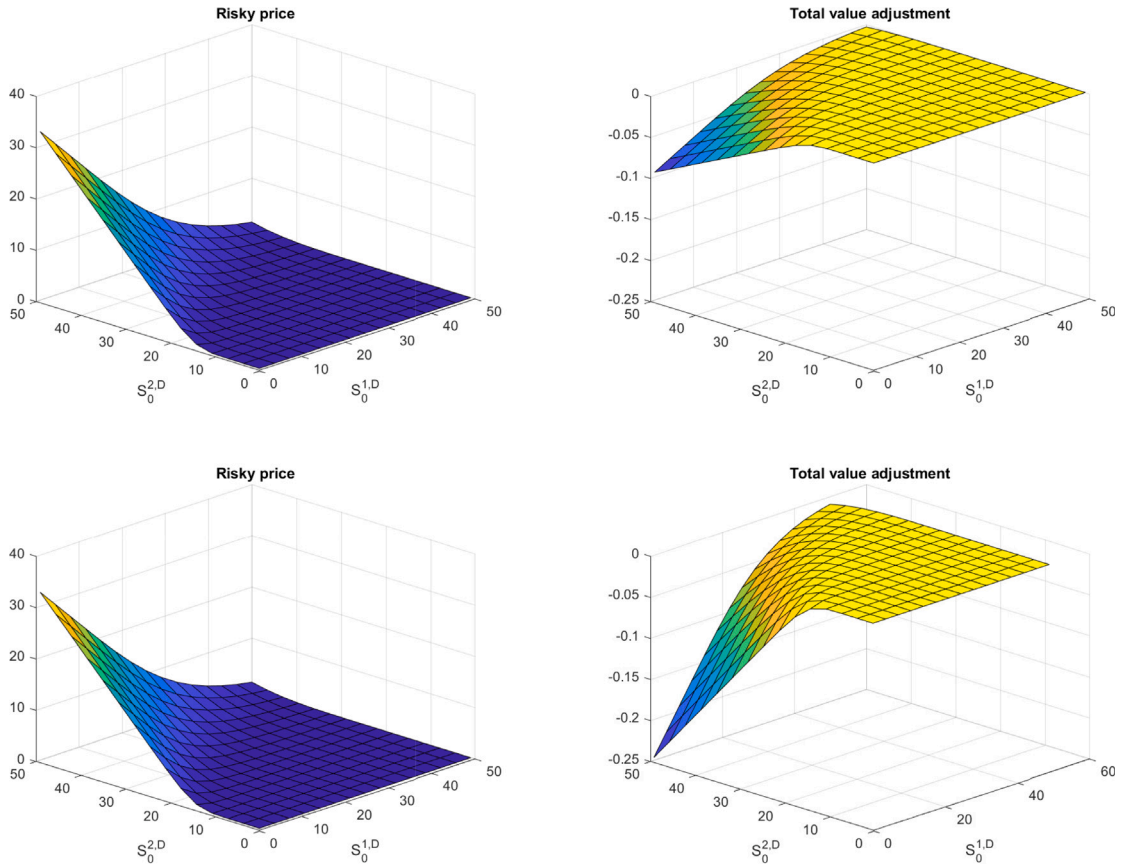

Fig. 6. Spread option in the linear case. Exponential Vasicek credit spread on the top and CIR credit spread on the bottom. Risky value on the left and XVA on the right (Test 5).

Table 13
Exchange option, nonlinear problem and deterministic exponential Vasicek credit spread. Comparison of Monte Carlo, multilevel Picard iteration and Lagrange-Galerkin methods. Total value adjustment (Test 6).

Total value adjustment						
$(S^{1,D}, S^{2,D})$	Monte Carlo		MPI		LG	
	SimpR	SimpT	$\rho = 4$	$\rho = 5$	$21 \times 21, 100$	$41 \times 41, 200$
(12, 9)	[−0.0410, −0.0389]	[−0.0222, −0.0211]	−0.0078	−0.0081	−0.0084	−0.0083
(12, 12)	[−0.0200, −0.0184]	[−0.0108, −0.0099]	−0.0037	−0.0039	−0.0041	−0.0040
(12, 15)	[−0.0087, −0.0076]	[−0.0047, −0.0041]	−0.0015	−0.0016	−0.0017	−0.0017
(30, 27)	[−0.0677, −0.0632]	[−0.0366, −0.0342]	−0.0134	−0.0133	−0.0137	−0.0134
(30, 30)	[−0.0500, −0.0460]	[−0.0270, −0.0248]	−0.0093	−0.0096	−0.0100	−0.0098
(30, 33)	[−0.0362, −0.0327]	[−0.0195, −0.0176]	−0.0067	−0.0069	−0.0072	−0.0070
(42, 39)	[−0.0871, −0.0810]	[−0.0471, −0.0437]	−0.0170	−0.0169	−0.0172	−0.0169
(42, 42)	[−0.0700, −0.0644]	[−0.0377, −0.0347]	−0.0131	−0.0134	−0.0135	−0.0132
(42, 45)	[−0.0557, −0.0506]	[−0.0300, −0.0273]	−0.0103	−0.0107	−0.0103	−0.0101

We show the empirical convergence of the multilevel Picard iteration method by plotting the relative approximations increments in Fig. 7.

4.2.2. Test 7: Linear problem, deterministic time dependent credit spread.

The results in the linear case with deterministic credit spread are reported in Table 15 and in Table 16.

The Lagrange-Galerkin method values with the finer mesh of 41×41 nodes and 200 time steps are not inside the Monte Carlo confidence intervals obtained with simple formulae, that are not reported, but are inside the confidence intervals obtained with composite formulae, except for the last considered point. In particular, the LG value in the last point, i.e., when $S^{1,D} = 42$ and $S^{2,D} = 45$, is slightly outside the Monte Carlo confidence interval with composite rectangular quadrature formula in the case of the exponential Vasicek credit spread, and is not in both confidence intervals in the case of the CIR credit spread. As pointed out when

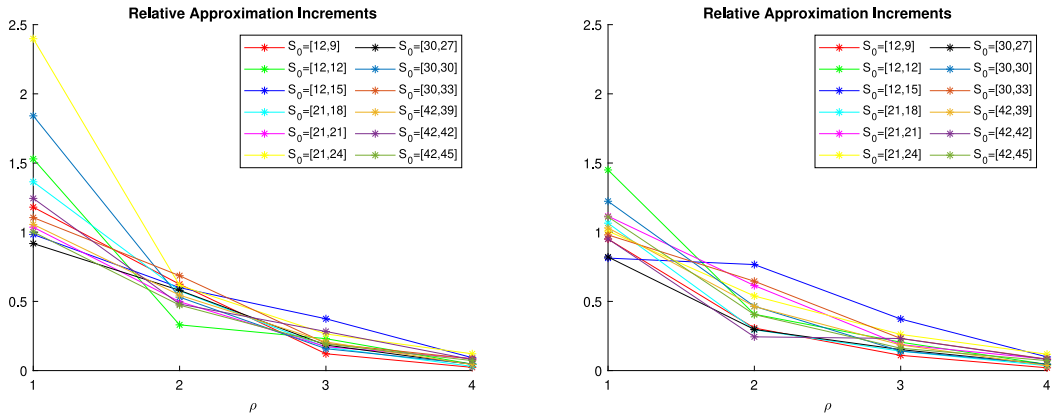

Fig. 7. Exchange option with deterministic credit spread. Convergence of the MPI with exponential Vasicek dynamics for credit spread on the left and CIR dynamics on the right.

Table 14
Exchange option, nonlinear problem and deterministic CIR credit spread. Comparison of Monte Carlo, multilevel Picard iteration and Lagrange-Galerkin methods. Total value adjustment (Test 6).

Total value adjustment						
$(S^{1,D}, S^{2,D})$	Monte Carlo		MPI		LG	
	SimpR	SimpT	$\rho = 4$	$\rho = 5$	$21 \times 21, 100$	$41 \times 41, 200$
$(12, 9)$	$[-0.0410, -0.0389]$	$[-0.0279, -0.0265]$	-0.0241	-0.0247	-0.0250	-0.0248
$(12, 12)$	$[-0.0200, -0.0184]$	$[-0.0135, -0.0125]$	-0.0115	-0.0118	-0.0121	-0.0119
$(12, 15)$	$[-0.0087, -0.0076]$	$[-0.0058, -0.0051]$	-0.0045	-0.0048	-0.0051	-0.0051
$(30, 27)$	$[-0.0677, -0.0632]$	$[-0.0460, -0.0429]$	-0.0411	-0.0405	-0.0407	-0.0403
$(30, 30)$	$[-0.0500, -0.0460]$	$[-0.0338, -0.0311]$	-0.0288	-0.0292	-0.0299	-0.0295
$(30, 33)$	$[-0.0362, -0.0327]$	$[-0.0245, -0.0221]$	-0.0206	-0.0209	-0.0215	-0.0212
$(42, 39)$	$[-0.0871, -0.0810]$	$[-0.0591, -0.0549]$	-0.0525	-0.0515	-0.0512	-0.0506
$(42, 42)$	$[-0.0700, -0.0644]$	$[-0.0474, -0.0436]$	-0.0404	-0.0407	-0.0401	-0.0397
$(42, 45)$	$[-0.0557, -0.0506]$	$[-0.0376, -0.0342]$	-0.0317	-0.0324	-0.0307	-0.0303

Table 15
Exchange option, linear problem and deterministic exponential Vasicek credit spread. Comparison of Monte Carlo and Lagrange-Galerkin methods. Total value adjustment (Test 7).

Total value adjustment				
$(S^{1,D}, S^{2,D})$	Monte Carlo		LG	
	CompR	CompT	$21 \times 21, 100$	$41 \times 41, 200$
$(12, 9)$	$[-0.0084, -0.0079]$	$[-0.0083, -0.0079]$	-0.0084	-0.0083
$(12, 12)$	$[-0.0040, -0.0037]$	$[-0.0040, -0.0037]$	-0.0041	-0.0040
$(12, 15)$	$[-0.0017, -0.0015]$	$[-0.0017, -0.0015]$	-0.0017	-0.0017
$(30, 27)$	$[-0.0137, -0.0128]$	$[-0.0136, -0.0127]$	-0.0137	-0.0134
$(30, 30)$	$[-0.0101, -0.0093]$	$[-0.0100, -0.0092]$	-0.0100	-0.0098
$(30, 33)$	$[-0.0073, -0.0066]$	$[-0.0072, -0.0066]$	-0.0072	-0.0070
$(42, 39)$	$[-0.0177, -0.0164]$	$[-0.0175, -0.0163]$	-0.0172	-0.0168
$(42, 42)$	$[-0.0142, -0.0130]$	$[-0.0140, -0.0129]$	-0.0135	-0.0132
$(42, 45)$	$[-0.0113, -0.0102]$	$[-0.0112, -0.0101]$	-0.0103	-0.0101

discussing about the results in the nonlinear case, this is due to the fact that the last point is too close to the spatial boundaries chosen in the LG method. Also, we can observe that each LG value is very close to the lower bound of the corresponding Monte Carlo confidence interval and that by refining the spatial and time meshes in the LG method the values become less negative. Therefore, we can expect that by using a finer mesh in the Lagrange-Galerkin method we can obtain values that are closer to the centres of the Monte Carlo confidence intervals.

4.2.3. Test 8: Nonlinear problem, stochastic credit spread.

We now consider the nonlinear case with stochastic credit spread and analyse how different initial values of the counterparty's credit spread affect the total value adjustment. In the case of stochastic spread of the counterparty, three stochastic factors are involved in the pricing of exchange options.

Table 16
Exchange option, linear problem and deterministic CIR credit spread. Comparison of Monte Carlo and Lagrange-Galerkin methods. Total value adjustment (Test 7).

Total value adjustment				
$(S^{1,D}, S^{2,D})$	Monte Carlo		LG	
	CompR	CompT	$21 \times 21, 100$	$41 \times 41, 200$
$(12, 9)$	$[-0.0252, -0.0239]$	$[-0.0252, -0.0239]$	-0.0249	-0.0248
$(12, 12)$	$[-0.0122, -0.0112]$	$[-0.0122, -0.0112]$	-0.0121	-0.0119
$(12, 15)$	$[-0.0053, -0.0046]$	$[-0.0053, -0.0046]$	-0.0051	-0.0051
$(30, 27)$	$[-0.0415, -0.0387]$	$[-0.0414, -0.0386]$	-0.0406	-0.0402
$(30, 30)$	$[-0.0305, -0.0281]$	$[-0.0305, -0.0280]$	-0.0298	-0.0294
$(30, 33)$	$[-0.0221, -0.0200]$	$[-0.0220, -0.0199]$	-0.0214	-0.0211
$(42, 39)$	$[-0.0533, -0.0496]$	$[-0.0532, -0.0495]$	-0.0510	-0.0505
$(42, 42)$	$[-0.0428, -0.0393]$	$[-0.0427, -0.0393]$	-0.0400	-0.0396
$(42, 45)$	$[-0.0340, -0.0309]$	$[-0.0339, -0.0308]$	-0.0306	-0.0302

Table 17
Exchange option, nonlinear problem and stochastic exponential Vasicek credit spread. Comparison of Monte Carlo and multilevel Picard iteration methods. Total value adjustment (Test 8).

Total value adjustment				
$(S^{2,D}, h)$	Monte Carlo		MPI	
	SimpR	SimpT	$\rho = 4$	$\rho = 5$
$(27, 0.010)$	$[-0.0273, -0.0254]$	$[-0.0191, -0.0176]$	-0.0130	-0.0133
$(27, 0.015)$	$[-0.0476, -0.0444]$	$[-0.0292, -0.0272]$	-0.0160	-0.0166
$(27, 0.020)$	$[-0.0677, -0.0632]$	$[-0.0393, -0.0366]$	-0.0183	-0.0185
$(27, 0.025)$	$[-0.0878, -0.0819]$	$[-0.0494, -0.0460]$	-0.0222	-0.0209
$(30, 0.010)$	$[-0.0201, -0.0185]$	$[-0.0142, -0.0130]$	-0.0103	-0.0103
$(30, 0.015)$	$[-0.0351, -0.0323]$	$[-0.0217, -0.0199]$	-0.0113	-0.0123
$(30, 0.020)$	$[-0.0500, -0.0460]$	$[-0.0292, -0.0268]$	-0.0141	-0.0142
$(30, 0.025)$	$[-0.0648, -0.0596]$	$[-0.0366, -0.0336]$	-0.0155	-0.0156
$(33, 0.010)$	$[-0.0145, -0.0131]$	$[-0.0104, -0.0094]$	-0.0072	-0.0075
$(33, 0.015)$	$[-0.0254, -0.0230]$	$[-0.0159, -0.0143]$	-0.0090	-0.0090
$(33, 0.020)$	$[-0.0362, -0.0327]$	$[-0.0212, -0.0191]$	-0.0101	-0.0102
$(33, 0.025)$	$[-0.0470, -0.0425]$	$[-0.0266, -0.0240]$	-0.0117	-0.0116

Table 18
Exchange option, nonlinear problem and stochastic CIR credit spread. Comparison of Monte Carlo and multilevel Picard iteration methods. Total value adjustment (Test 8).

Total value adjustment				
$(S^{2,D}, h)$	Monte Carlo		MPI	
	SimpR	SimpT	$\rho = 4$	$\rho = 5$
$(27, 0.010)$	$[-0.0273, -0.0254]$	$[-0.0227, -0.0211]$	-0.0206	-0.0210
$(27, 0.015)$	$[-0.0476, -0.0444]$	$[-0.0361, -0.0335]$	-0.0324	-0.0332
$(27, 0.020)$	$[-0.0677, -0.0632]$	$[-0.0493, -0.0458]$	-0.0439	-0.0439
$(27, 0.025)$	$[-0.0878, -0.0819]$	$[-0.0624, -0.0581]$	-0.0584	-0.0558
$(30, 0.010)$	$[-0.0201, -0.0185]$	$[-0.0170, -0.0156]$	-0.0160	-0.0160
$(30, 0.015)$	$[-0.0351, -0.0323]$	$[-0.0269, -0.0246]$	-0.0227	-0.0245
$(30, 0.020)$	$[-0.0500, -0.0460]$	$[-0.0366, -0.0336]$	-0.0333	-0.0331
$(30, 0.025)$	$[-0.0648, -0.0596]$	$[-0.0463, -0.0425]$	-0.0410	-0.0411
$(33, 0.010)$	$[-0.0145, -0.0131]$	$[-0.0125, -0.0112]$	-0.0112	-0.0115
$(33, 0.015)$	$[-0.0254, -0.0230]$	$[-0.0197, -0.0177]$	-0.0176	-0.0177
$(33, 0.020)$	$[-0.0362, -0.0327]$	$[-0.0267, -0.0241]$	-0.0234	-0.0236
$(33, 0.025)$	$[-0.0470, -0.0425]$	$[-0.0338, -0.0304]$	-0.0303	-0.0301

We fix the initial value of the first underlying asset to $S^{1,D} = 30$ and choose the values of $S^{2,D}$ equal to 27, 30, 33, so that to consider the in the money, at the money and out of the money cases, respectively. The results are shown in Table 17 for the exponential Vasicek credit spread and in Table 18 for the CIR credit spread. The Monte Carlo method with simple quadrature formulae does not approximate well enough the total value adjustment, overestimating, in absolute terms, the XVA with respect the multilevel Picard iterations results, that we take as reference values. As expected, the XVA is affected by the increasing of the probability of the counterparty's default: it becomes more negative when it is more likely that the counterparty defaults. Also, we can see that the total value adjustment is more negative under the assumption of a CIR credit spread. This is evident also in Fig. 8 especially for low initial values of $S^{2,D}$ and large values of the counterparty's intensity of default.

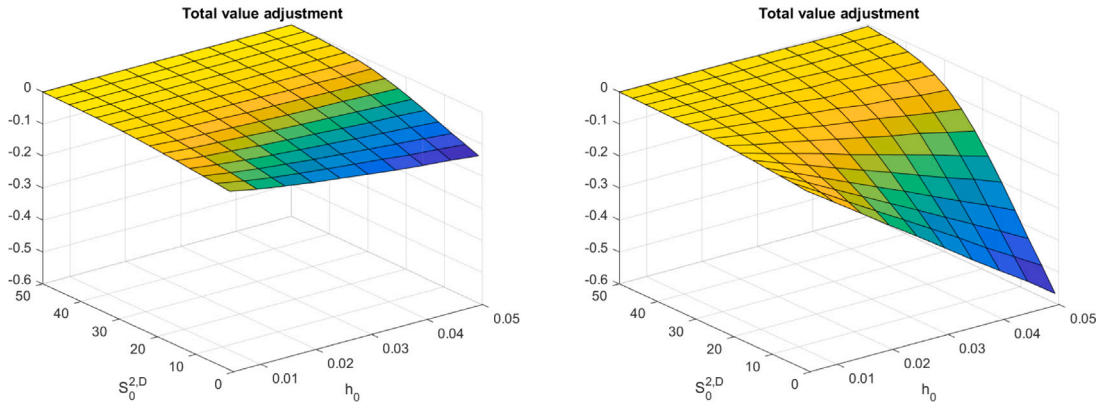

Fig. 8. Exchange option in the nonlinear case. Total value adjustment with both exponential Vasicek credit spread (on the left) and CIR credit spread (on the right) (Test 8).

Table 19
Exchange option, linear problem and stochastic exponential Vasicek credit spread. Comparison of different quadrature formulae in Monte Carlo method. Total value adjustment (Test 9).

Total value adjustment				
$(S^{2,D}, h)$	Monte Carlo			
	SimpR	SimpT	CompR	CompT
(27, 0.010)	[−0.0109, −0.0096]	[−0.0191, −0.0177]	[−0.0140, −0.0129]	[−0.0140, −0.0128]
(27, 0.015)	[−0.0109, −0.0097]	[−0.0294, −0.0273]	[−0.0170, −0.0156]	[−0.0169, −0.0156]
(27, 0.020)	[−0.0110, −0.0097]	[−0.0396, −0.0369]	[−0.0196, −0.0180]	[−0.0195, −0.0179]
(27, 0.025)	[−0.0110, −0.0097]	[−0.0499, −0.0465]	[−0.0219, −0.0202]	[−0.0217, −0.0201]
(30, 0.010)	[−0.0084, −0.0073]	[−0.0142, −0.0130]	[−0.0107, −0.0096]	[−0.0107, −0.0096]
(30, 0.015)	[−0.0085, −0.0074]	[−0.0218, −0.0200]	[−0.0129, −0.0117]	[−0.0128, −0.0116]
(30, 0.020)	[−0.0085, −0.0074]	[−0.0294, −0.0269]	[−0.0148, −0.0134]	[−0.0147, −0.0133]
(30, 0.025)	[−0.0085, −0.0074]	[−0.0369, −0.0339]	[−0.0165, −0.0150]	[−0.0164, −0.0149]
(33, 0.010)	[−0.0064, −0.0054]	[−0.0104, −0.0094]	[−0.0080, −0.0071]	[−0.0079, −0.0070]
(33, 0.015)	[−0.0064, −0.0055]	[−0.0159, −0.0143]	[−0.0096, −0.0085]	[−0.0095, −0.0085]
(33, 0.020)	[−0.0065, −0.0055]	[−0.0214, −0.0193]	[−0.0110, −0.0098]	[−0.0109, −0.0097]
(33, 0.025)	[−0.0065, −0.0055]	[−0.0269, −0.0242]	[−0.0122, −0.0109]	[−0.0121, −0.0108]

Table 20
Exchange option, linear problem and stochastic CIR credit spread. Comparison of different quadrature formulae in Monte Carlo method. Total value adjustment (Test 9).

Total value adjustment				
$(S^{2,D}, h)$	Monte Carlo			
	SimpR	SimpT	CompR	CompT
(27, 0.010)	[−0.0181, −0.0165]	[−0.0227, −0.0211]	[−0.0220, −0.0203]	[−0.0220, −0.0203]
(27, 0.015)	[−0.0244, −0.0224]	[−0.0361, −0.0336]	[−0.0340, −0.0315]	[−0.0339, −0.0315]
(27, 0.020)	[−0.0306, −0.0281]	[−0.0494, −0.0460]	[−0.0459, −0.0426]	[−0.0458, −0.0425]
(27, 0.025)	[−0.0366, −0.0337]	[−0.0627, −0.0583]	[−0.0576, −0.0536]	[−0.0575, −0.0535]
(30, 0.010)	[−0.0139, −0.0125]	[−0.0170, −0.0155]	[−0.0165, −0.0151]	[−0.0165, −0.0150]
(30, 0.015)	[−0.0186, −0.0168]	[−0.0269, −0.0246]	[−0.0254, −0.0232]	[−0.0254, −0.0232]
(30, 0.020)	[−0.0232, −0.0210]	[−0.0367, −0.0337]	[−0.0342, −0.0313]	[−0.0342, −0.0313]
(30, 0.025)	[−0.0277, −0.0252]	[−0.0465, −0.0427]	[−0.0429, −0.0393]	[−0.0429, −0.0392]
(33, 0.010)	[−0.0105, −0.0092]	[−0.0125, −0.0112]	[−0.0122, −0.0109]	[−0.0122, −0.0109]
(33, 0.015)	[−0.0139, −0.0123]	[−0.0197, −0.0177]	[−0.0187, −0.0168]	[−0.0186, −0.0167]
(33, 0.020)	[−0.0173, −0.0154]	[−0.0268, −0.0242]	[−0.0251, −0.0225]	[−0.0250, −0.0225]
(33, 0.025)	[−0.0206, −0.0184]	[−0.0339, −0.0306]	[−0.0314, −0.0282]	[−0.0313, −0.0282]

4.2.4. Test 9: Linear problem, stochastic credit spread.

When considering the linear problem (results in Table 19 for the exponential Vasicek credit spread and in Table 20 for the CIR credit spread) we can draw the same conclusions as for the nonlinear problem.

Fig. 9 shows the risky price and the XVA. Under the assumption of a CIR credit spread, it can be seen that when the option is out of the money the total value adjustment remains small, even increasing the probability of the counterparty's default, although when the option is in the money the total value adjustment decays quickly when increasing the counterparty's credit spread h. This is less clear in the case of an exponential Vasicek credit spread, because XVA is smaller, in absolute terms.

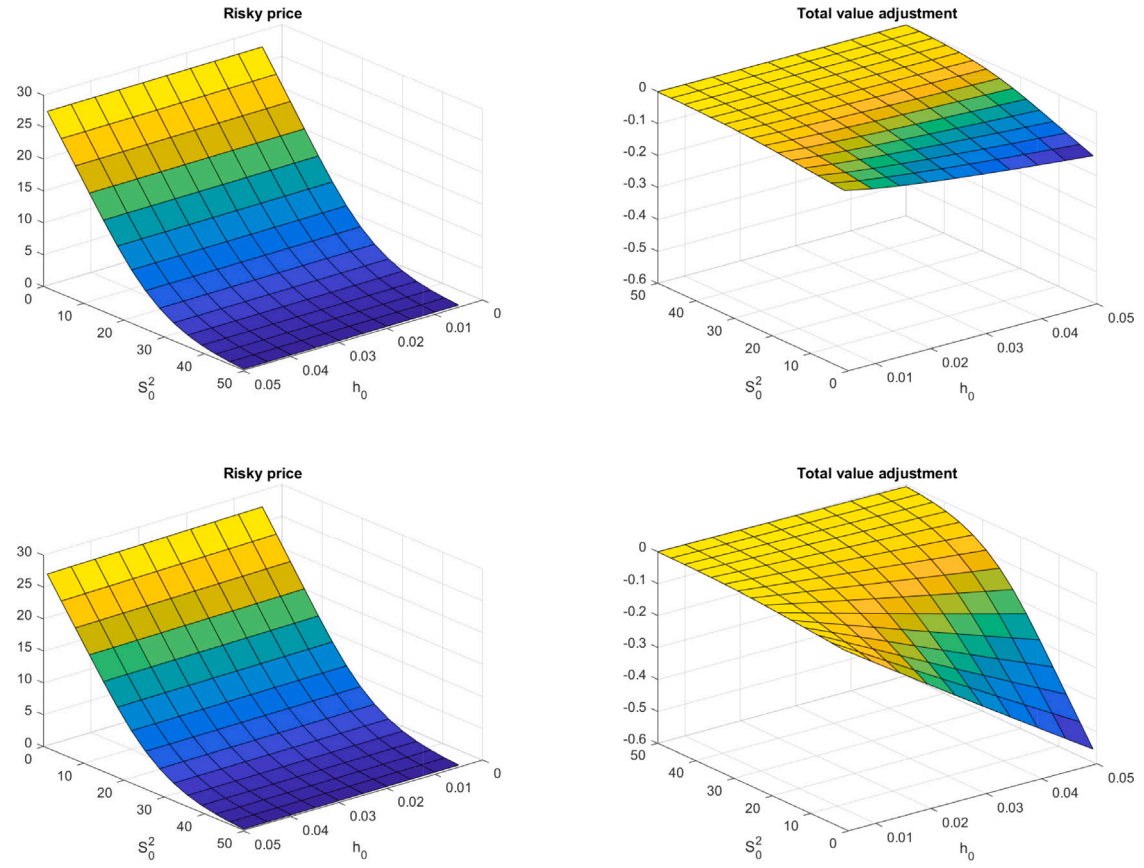

Fig. 9. Exchange option in the linear case. Exponential Vasicek credit spread on the top and CIR credit spread on the bottom. Risky value on the left and XVA on the right (Test 9).

4.3. Sum of call options

Finally, we assume the hedger buys from the counterparty a portfolio of European call options in different currencies, so that the portfolio payoff function is the sum of the payoff functions of the involved call options, i.e.

$$G(t, S^1, \dots, S^N) = \sum_{i=1}^{N} (X^{D,C_i} S^i - K^i)^+ ,$$

where $S^1, \dots, S^N$ are the N assets respectively denominated in currencies $C_1, \dots, C_N$, and $K^1, \dots, K^N$ are the strike values given in the domestic currency D.

In our numerical tests we first assume the derivative is written on two underlying assets, i.e. $N = 2$, and we use data reported listed in Table 1. The strike values are set to $K^1 = 15$ and $K^2 = 12$. When considering more than two underlying assets, the values of S_0^i, r^i, q^i, σ^{S^i}, K^i, for $i = 1, \dots, N$, are taken form Table 25.

As in the previous examples, we assume that the counterparty is defaultable, while the hedger is default-free. Hence, only the hedger will charge the counterparty an adjustment on the trade, thus reducing the value of the derivative with respect to the risk-free setting.

4.3.1. Test 10: Nonlinear problem, deterministic time dependent credit spread.

We first consider a sum of two call options in the nonlinear case with the deterministic time dependent credit spread and show the numerical results in Table 21 and in Table 22, whereas the convergence of the multilevel Picard iteration method is shown in Fig. 10. We have chosen the initial value of the underlying assets so that for each of the two call options we consider the in the money, the at the money and the out of the money cases and test all the possible combinations. As in the previously analysed products, we can see that multilevel Picard iteration method results are close to the ones obtained with Lagrange-Galerkin method, especially when taking $\rho = 5$ in the MPI and a finer mesh in the LG.

Table 21
Sum of call options, nonlinear problem and deterministic exponential Vasicek credit spread. Comparison of Monte Carlo, multilevel Picard iteration and Lagrange-Galerkin methods. Total value adjustment (Test 10).

Total value adjustment						
$(S^{1,D}, S^{2,D})$	Monte Carlo		MPI		LG	
	SimpR	SimpT	$\rho = 4$	$\rho = 5$	$21 \times 21, 100$	$41 \times 41, 200$
(12, 9)	[−0.0087, −0.0076]	[−0.0047, −0.0041]	−0.0015	−0.0016	−0.0016	−0.0017
(12, 12)	[−0.0206, −0.0191]	[−0.0111, −0.0103]	−0.0037	−0.0040	−0.0042	−0.0042
(12, 15)	[−0.0480, −0.0459]	[−0.0261, −0.0250]	−0.0095	−0.0095	−0.0099	−0.0098
(15, 9)	[−0.0251, −0.0231]	[−0.0135, −0.0125]	−0.0050	−0.0048	−0.0050	−0.0050
(15, 12)	[−0.0368, −0.0345]	[−0.0200, −0.0187]	−0.0071	−0.0073	−0.0077	−0.0075
(15, 15)	[−0.0642, −0.0614]	[−0.0349, −0.0334]	−0.0125	−0.0128	−0.0134	−0.0131
(18, 9)	[−0.0503, −0.0474]	[−0.0273, −0.0257]	−0.0098	−0.0099	−0.0102	−0.0101
(18, 12)	[−0.0620, −0.0588]	[−0.0337, −0.0319]	−0.0121	−0.0122	−0.0128	−0.0126
(18, 15)	[−0.0893, −0.0857]	[−0.0486, −0.0467]	−0.0175	−0.0179	−0.0185	−0.0182

Table 22
Sum of call options, nonlinear problem and deterministic CIR credit spread. Comparison of Monte Carlo, multilevel Picard iteration and Lagrange-Galerkin methods. Total value adjustment (Test 10).

Total value adjustment						
$(S^{1,D}, S^{2,D})$	Monte Carlo		MPI		LG	
	SimpR	SimpT	$\rho = 4$	$\rho = 5$	$21 \times 21, 100$	$41 \times 41, 200$
(12, 9)	[−0.0087, −0.0076]	[−0.0059, −0.0051]	−0.0047	−0.0049	−0.0048	−0.0051
(12, 12)	[−0.0206, −0.0191]	[−0.0140, −0.0129]	−0.0114	−0.0121	−0.0125	−0.0126
(12, 15)	[−0.0480, −0.0459]	[−0.0328, −0.0314]	−0.0292	−0.0290	−0.0295	−0.0294
(15, 9)	[−0.0251, −0.0231]	[−0.0170, −0.0156]	−0.0155	−0.0147	−0.0150	−0.0151
(15, 12)	[−0.0368, −0.0345]	[−0.0251, −0.0235]	−0.0219	−0.0221	−0.0228	−0.0225
(15, 15)	[−0.0642, −0.0614]	[−0.0438, −0.0419]	−0.0385	−0.0390	−0.0398	−0.0393
(18, 9)	[−0.0503, −0.0474]	[−0.0342, −0.0322]	−0.0301	−0.0302	−0.0303	−0.0303
(18, 12)	[−0.0620, −0.0588]	[−0.0422, −0.0401]	−0.0371	−0.0372	−0.0382	−0.0378
(18, 15)	[−0.0893, −0.0857]	[−0.0610, −0.0586]	−0.0540	−0.0544	−0.0551	−0.0546

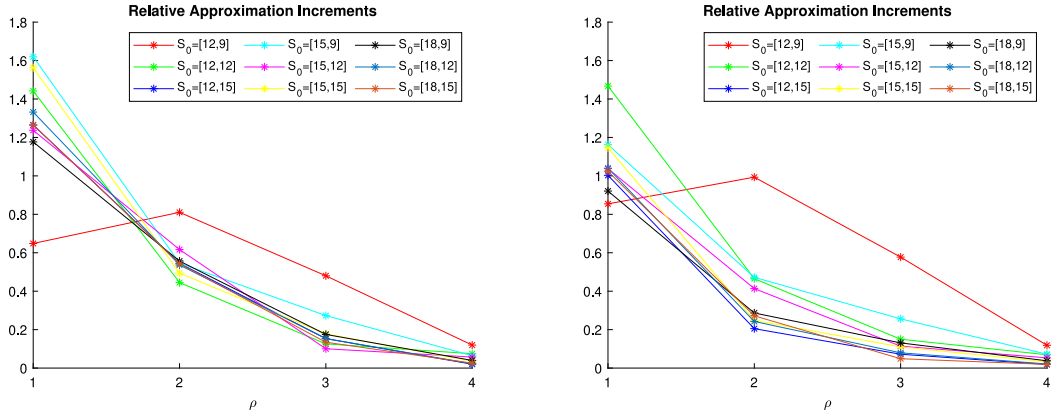

Fig. 10. Sum of call options with deterministic credit spread. Convergence of the MPI with exponential Vasicek dynamics for credit spread on the left and CIR dynamics on the right.

4.3.2. Test 11: Linear problem, deterministic time dependent credit spread.

For the linear case with deterministic credit spread, XVA numerical results are shown in Table 23 for the exponential Vasicek dynamics and in Table 24 for the CIR dynamics. In the first case, when taking a mesh of 21×21 nodes and 100 time steps in the Lagrange-Galerkin method, there are some values outside the corresponding Monte Carlo confidence intervals. However, when taking a finer mesh, the resulting XVA values are inside or on the lower bound of Monte Carlo confidence intervals obtained with the rectangular composite formula. When considering the trapezoidal composite formula, there are some LG values that are slightly outside the corresponding Monte Carlo confidence intervals. As already pointed out in the case of the exchange option, the use of an even more refined mesh probably makes the Lagrange-Galerkin values less negative and, therefore, closer to the centres of the confidence intervals. In the case of the CIR dynamics, the Lagrange-Galerkin results with both the considered discretization meshes are inside the Monte Carlo confidence intervals, except for the point $(S^{1,D}, S^{1,D}) = (15, 15)$, where the XVA obtained with the coarser mesh is slightly outside the confidence intervals.

Table 23
Sum of call options, linear problem and deterministic exponential Vasicek credit spread. Comparison of Monte Carlo and Lagrange-Galerkin methods. Total value adjustment (Test 11).

Total value adjustment				
$(S^{1,D}, S^{2,D})$	Monte Carlo		LG	
	CompR	CompT	$21 \times 21, 100$	$41 \times 41, 200$
$(12, 9)$	$[-0.0018, -0.0015]$	$[-0.0017, -0.0015]$	-0.0016	-0.0017
$(12, 12)$	$[-0.0042, -0.0039]$	$[-0.0041, -0.0038]$	-0.0042	-0.0042
$(12, 15)$	$[-0.0098, -0.0094]$	$[-0.0097, -0.0093]$	-0.0099	-0.0098
$(15, 9)$	$[-0.0051, -0.0047]$	$[-0.0050, -0.0046]$	-0.0050	-0.0050
$(15, 12)$	$[-0.0075, -0.0070]$	$[-0.0074, -0.0070]$	-0.0077	-0.0075
$(15, 15)$	$[-0.0131, -0.0125]$	$[-0.0130, -0.0124]$	-0.0133	-0.0131
$(18, 9)$	$[-0.0102, -0.0096]$	$[-0.0101, -0.0096]$	-0.0102	-0.0101
$(18, 12)$	$[-0.0126, -0.0120]$	$[-0.0125, -0.0119]$	-0.0128	-0.0126
$(18, 15)$	$[-0.0182, -0.0175]$	$[-0.0181, -0.0174]$	-0.0185	-0.0182

Table 24
Sum of call options, linear problem and deterministic CIR credit spread. Comparison of Monte Carlo and Lagrange-Galerkin methods. Total value adjustment (Test 11).

Total value adjustment				
$(S^{1,D}, S^{2,D})$	Monte Carlo		LG	
	CompR	CompT	$21 \times 21, 100$	$41 \times 41, 200$
$(12, 9)$	$[-0.0053, -0.0046]$	$[-0.0053, -0.0046]$	-0.0047	-0.0051
$(12, 12)$	$[-0.0126, -0.0117]$	$[-0.0126, -0.0117]$	-0.0125	-0.0125
$(12, 15)$	$[-0.0296, -0.0283]$	$[-0.0295, -0.0282]$	-0.0294	-0.0293
$(15, 9)$	$[-0.0153, -0.0141]$	$[-0.0153, -0.0141]$	-0.0149	-0.0150
$(15, 12)$	$[-0.0226, -0.0212]$	$[-0.0226, -0.0212]$	-0.0227	-0.0225
$(15, 15)$	$[-0.0396, -0.0379]$	$[-0.0395, -0.0378]$	-0.0397	-0.0392
$(18, 9)$	$[-0.0309, -0.0291]$	$[-0.0308, -0.0290]$	-0.0302	-0.0302
$(18, 12)$	$[-0.0381, -0.0362]$	$[-0.0381, -0.0361]$	-0.0380	-0.0377
$(18, 15)$	$[-0.0551, -0.0529]$	$[-0.0549, -0.0528]$	-0.0550	-0.0545

Table 25
Data for the sum of call options. For $N = 2, 4, 8, 16, 32$ we respectively consider the N first rows of the table.

i	$S^{i,D}$	r^i	q^i	σ^{S^i}	K^i	i	$S^{i,D}$	r^i	q^i	σ^{S^i}	K^i
1	11	0.020	0.030	0.300	15	17	11	0.018	0.025	0.324	10
2	13	0.020	0.010	0.200	12	18	13	0.006	0.032	0.288	11
3	13	0.037	0.011	0.289	15	19	15	0.001	0.035	0.306	13
4	14	0.026	0.024	0.299	10	20	14	0.017	0.033	0.277	13
5	14	0.024	0.024	0.277	13	21	10	0.026	0.011	0.325	13
6	11	0.008	0.033	0.271	13	22	13	0.014	0.020	0.308	11
7	10	0.002	0.032	0.201	10	23	12	0.018	0.013	0.330	15
8	13	0.014	0.016	0.210	10	24	10	0.015	0.035	0.230	15
9	10	0.017	0.022	0.265	13	25	15	0.018	0.014	0.245	12
10	14	0.021	0.017	0.265	15	26	15	0.023	0.013	0.271	14
11	13	0.006	0.034	0.228	10	27	11	0.010	0.021	0.274	14
12	15	0.011	0.029	0.279	12	28	13	0.022	0.012	0.291	12
13	15	0.029	0.012	0.290	15	29	12	0.008	0.030	0.323	11
14	11	0.013	0.028	0.308	12	30	12	0.003	0.045	0.279	11
15	15	0.008	0.037	0.246	12	31	13	0.002	0.035	0.341	11
16	14	0.033	0.011	0.261	11	32	13	0.026	0.024	0.309	12

We now consider the sum of call options on different numbers N of assets in their corresponding currencies. Table 25 shows data for the case of $N = 32$ assets. Note that when considering a number of assets lower than 32, we use the data of rows $i = 1, \dots, N$ appearing in Table 25 (i.e., for the case of 2 assets we consider the rows $i = 1, 2$, and so on for 4, 8, 16 and 32 assets).

Table 26 shows the risk-free prices, that are obviously independent of the counterparty's credit spread and of the choice of the mark-to-market value. With the chosen data, the risk-free price increases by increasing the number of the underlying assets, so we expect that the XVA becomes more negative. The total value adjustment is analysed in the next two tests both in the nonlinear case and in the linear case.

4.3.3. Test 12: Nonlinear problem, stochastic credit spread

We assume the counterparty's credit spread is stochastic and that the mark-to-market value is equal to the risky derivative value (nonlinear case).

Tables 27 and 28 show the total value adjustment for different numbers of underlying assets. In particular, we show the average value of XVA on $N_{runs} = 10$ runs of the multilevel Picard iteration method. Also, the tables report the elapsed computational time

Table 26
Sum of call options. Monte Carlo confidence intervals. Risk-free value.

Risk-free value	
N	Monte Carlo
2	[1.9330, 2.0468]
4	[7.1207, 7.3713]
8	[13.5861, 13.9660]
16	[30.8413, 31.4230]
32	[60.2779, 61.1494]

Table 27
Sum of call options, nonlinear problem and stochastic exponential Vasicek credit spread. Multilevel Picard iteration results. Total value adjustment and elapsed time in seconds (Test 12).

Total value adjustment			Elapsed time		
N	MPI		N	MPI	
	$\rho = 4$	$\rho = 5$		$\rho = 4$	$\rho = 5$
2	−0.0057	−0.0058	2	11.1905	3816.6932
4	−0.0216	−0.0215	4	16.7175	4775.5968
8	−0.0400	−0.0409	8	26.4006	7375.3050
16	−0.0912	−0.0913	16	42.3238	12 573.8821
32	−0.1778	−0.1795	32	75.8329	22 500.3082

Table 28
Sum of call options, nonlinear problem and stochastic CIR credit spread. Multilevel Picard iteration results. Total value adjustment and elapsed time in seconds (Test 12).

Total value adjustment			Elapsed time		
N	MPI		N	MPI	
	$\rho = 4$	$\rho = 5$		$\rho = 4$	$\rho = 5$
2	−0.0150	−0.0151	2	12.1386	3596.6193
4	−0.0561	−0.0556	4	15.8039	4988.5962
8	−0.1048	−0.1059	8	27.1096	7512.3959
16	−0.2391	−0.2379	16	41.6914	12 348.0835
32	−0.4649	−0.4661	32	75.2775	21 826.0707

for $N_{runs} = 10$ runs of the MPI. The elapsed computational time does not depend on the dynamics chosen for the credit spread, but increases by increasing the value of the parameter ρ. In fact, we recall that the number of simulations is fixed to $m_{n,l,\rho} = \rho^{n-l}$ and the number of rectangles is chosen to be ρ^{n-l}, so that larger values of ρ correspond to larger numbers of simulations and of discretization nodes.

Fig. 11 shows that the empirical convergence of the multilevel Picard iteration for different numbers of assets.

4.3.4. Test 13: Linear problem, stochastic credit spread

Finally, we consider the sum of up to $N = 32$ call options in the linear case and report the computed total value adjustment and the elapsed time in Table 29 and in Table 30. Results are obtained by using the Monte Carlo method with composite quadrature formulae and the 99% confidence intervals are reported. As in the nonlinear case, the XVA is more negative for larger values of N. The elapsed time does not depend on the choice of the credit spread dynamics and the trapezoidal formula is a little more time-consuming than the rectangular formula.

5. Conclusions

We have addressed the modelling and the computation of the total value adjustment in a multi-currency setting by considering a derivative written on assets denominated in foreign currencies. We have assumed that the foreign exchange rates are deterministic, the derivative is partially collateralized in cash in a foreign currency and the counterparty's intensity of default follows a mean reversion process, either an exponential Vasicek or a CIR one. Last two assumptions are new with respect to a previous work of the authors.

The portfolio replication and the dynamic hedging methodologies have provided the formulation of XVA pricing problem in terms of nonlinear and linear PDEs. Moreover, the use of Feynman–Kac formulas has provided the equivalent formulations in terms of expectations that allow to apply Monte Carlo simulation techniques to the corresponding nonlinear and linear models.

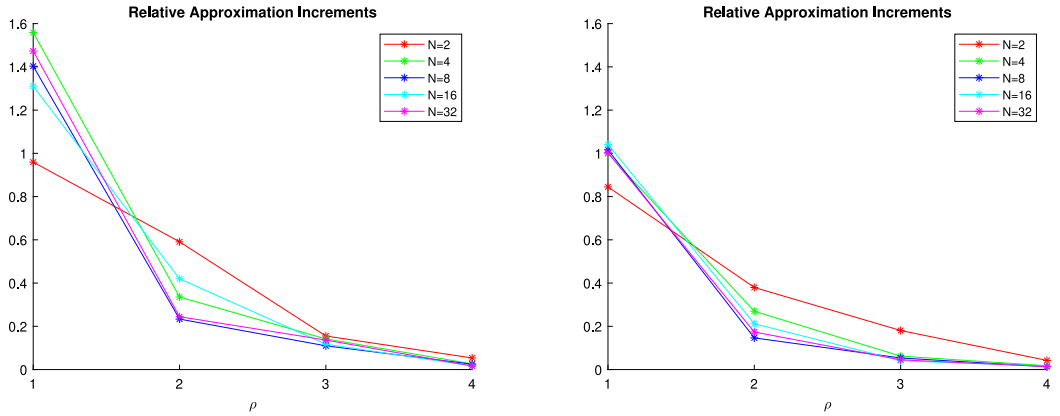

Fig. 11. Sum of call options with stochastic credit spread. Convergence of the MPI with exponential Vasicek dynamics for credit spread on the left and CIR dynamics on the right.

Table 29
Sum of call options, linear problem and stochastic exponential Vasicek credit spread. Comparison of different quadrature formulae in Monte Carlo method. Total value adjustment and elapsed time (Test 13).

Total value adjustment			Elapsed time		
N	Monte Carlo		N	Monte Carlo	
	CompR	CompT		CompR	CompT
2	[−0.0061, −0.0057]	[−0.0060, −0.0056]	2	0.5384	0.5389
4	[−0.0222, −0.0212]	[−0.0220, −0.0211]	4	0.6200	0.6814
8	[−0.0415, −0.0399]	[−0.0411, −0.0396]	8	0.8646	0.8936
16	[−0.0922, −0.0896]	[−0.0915, −0.0889]	16	2.6761	2.6853
32	[−0.1809, −0.1762]	[−0.1796, −0.1748]	32	3.4442	3.5099

Table 30
Sum of call options, linear problem and stochastic CIR credit spread. Comparison of different quadrature formulae in Monte Carlo method. Total value adjustment and elapsed time (Test 13).

Total value adjustment			Elapsed time		
N	Monte Carlo		N	Monte Carlo	
	CompR	CompT		CompR	CompT
2	[−0.0156, −0.0147]	[−0.0155, −0.0146]	2	0.5177	0.5528
4	[−0.0564, −0.0544]	[−0.0563, −0.0542]	4	0.6640	0.6759
8	[−0.1063, −0.1031]	[−0.1061, −0.1029]	8	0.8809	0.9064
16	[−0.2380, −0.2328]	[−0.2375, −0.2323]	16	2.5279	2.5478
32	[−0.4647, −0.4562]	[−0.4637, −0.4552]	32	3.7823	3.7983

Next, we have numerically solved the total value adjustment pricing PDEs by applying the Lagrange-Galerkin method under the assumption that the counterparty's credit spread is a deterministic function of time and the derivative is written on two underlying assets. From the comparison between the results obtained with Lagrange-Galerkin method and those computed with probabilistic techniques, we have deduced that in the nonlinear case the multilevel Picard iteration method results can be taken as reference values, whereas in the linear case we can consider the Monte Carlo confidence intervals obtained by using composite quadrature formulae for the approximation of the integral in the total value adjustment formulae.

Finally, as expected we have illustrated that the total value adjustment is more negative when the derivative is more valuable and that it becomes more and more negative by increasing the counterparty's probability of default.

Declaration of competing interest

The authors declare that they have no known competing financial interests or personal relationships that could have appeared to influence the work reported in this paper.

Data availability

No data was used for the research described in the article.

Acknowledgements

This work has been funded by EU H2020-MSCA-ITN-2018 (ABC-EU-XVA Grant Agreement 813261), Spanish Ministry of Science and Innovation (Grant PID2019-108584RB-I00) and by Galician Government (Grant ED431C2018/033), both including FEDER financial support. Authors also acknowledge the support received from the Centro de Investigación de Galicia (CITIC), Spain, funded by Xunta de Galicia and the European Union (European Regional Development Fund, Galicia 2014–2020 Program), by grant ED431G 2019/01. The authors also want to thank the anonymous referees for their insightful comments and suggestions, which have helped to improve the original manuscript.

Appendix. Analysis of boundary conditions

Following [33], we introduce the following subsets of $\partial\Omega^*$ in terms of the vector $\mathbf{m}$, orthogonal to the boundary and pointing inwards Ω^*:

$$\Sigma^0 = \left\{ x \in \partial\Omega^* \ : \ \sum_{i,j=0}^{2} a^*_{ij} m_i m_j = 0 \right\}, \quad \Sigma^1 = \partial\Omega^* - \Sigma^0,$$
$$\Sigma^2 = \left\{ x \in \Sigma^0 \ : \ \sum_{i=0}^{2} \left(b^*_i - \sum_{j=0}^{2} \frac{\partial a^*_{ij}}{\partial x_j} \right) m_i < 0 \right\}.$$

and we need to impose boundary conditions on $\Sigma^1 \cup \Sigma^2$.

Tables 31 and 32 summarize the values we need to identify the sets Σ^0, Σ^1 and Σ^2. Note that $y_{,j}$ denotes a partial derivative of y with respect to x_j and Euler summation on repeated indices is used. We assume $r^i - q^i > 0$ for $i = 1, 2$. From them, we deduce:

$$\Sigma^0 = \Gamma_0^- \cup \Gamma_0^+ \cup \Gamma_1^- \cup \Gamma_2^-, \quad \Sigma^1 = \Gamma_1^+ \cup \Gamma_2^+, \quad \Sigma^2 = \Gamma_0^-,$$

and, following [32,33], we have to impose conditions on $\Sigma^1 \cup \Sigma^2 = \Gamma_0^- \cup \Gamma_1^+ \cup \Gamma_2^+$.

According to the stated notation, $x_0 = \tau$ and Γ_0^- corresponds to the initial condition; thus, we need to impose boundary conditions on the right ($S^1 = S^1_\infty$) and upper ($S^2 = S^2_\infty$) boundaries of Ω.

Table 31
Analysis of boundary conditions [32].

	$\Gamma_0^{*,-}$	$\Gamma_0^{*,+}$
$\mathbf{m}$	$(1,0,0)$	$(-1,0,0)$
$a^*_{00} m_0 m_0$	0	0
$a^*_{01} m_0 m_1$	0	0
$a^*_{02} m_0 m_2$	0	0
$a^*_{10} m_1 m_0$	0	0
$a^*_{11} m_1 m_1$	0	0
$a^*_{12} m_1 m_2$	0	0
$a^*_{20} m_2 m_0$	0	0
$a^*_{21} m_2 m_1$	0	0
$a^*_{22} m_2 m_2$	0	0
$\sum_{i,j=0}^{1} a^*_{ij} m_i m_j$	0	0
$a^*_{00,0}$	0	0
$a^*_{01,1}$	0	0
$a^*_{02,2}$	0	0
$a^*_{10,0}$	0	0
$a^*_{11,1}$	$(\sigma^{S^1})^2 x_1$	$(\sigma^{S^1})^2 x_1$
$a^*_{12,2}$	$\frac{1}{2}\rho^{S^1 S^2}\sigma^{S^1}\sigma^{S^2} x_1$	$\frac{1}{2}\rho^{S^1 S^2}\sigma^{S^1}\sigma^{S^2} x_1$
$a^*_{20,0}$	0	0
$a^*_{21,1}$	$\frac{1}{2}\rho^{S^1 S^2}\sigma^{S^1}\sigma^{S^2} x_2$	$\frac{1}{2}\rho^{S^1 S^2}\sigma^{S^1}\sigma^{S^2} x_2$
$a^*_{22,2}$	$(\sigma^{S^2})^2 x_2$	$(\sigma^{S^2})^2 x_2$
b^*_0	-1	-1
b^*_1	$(r^1 - q^1) x_1$	$(r^1 - q^1) x_1$
b^*_2	$(r^2 - q^2) x_2$	$(r^2 - q^2) x_2$
$(b^*_0 - a^*_{0j,j}) m_0$	-1	1
$(b^*_1 - a^*_{1j,j}) m_1$	0	0
$(b^*_2 - a^*_{2j,j}) m_2$	0	0
$\sum_{i=0}^{2} (b^*_i - a^*_{ij,j}) m_i$	-1	1

Table 32
Analysis of boundary conditions [32].

	$\Gamma_1^{*,-}$	$\Gamma_1^{*,+}$	$\Gamma_2^{*,-}$	$\Gamma_2^{*,+}$
m	$(0,1,0)$	$(0,-1,0)$	$(0,0,1)$	$(0,0,-1)$
$a^*_{00}m_0m_0$	0	0	0	0
$a^*_{01}m_0m_1$	0	0	0	0
$a^*_{02}m_0m_2$	0	0	0	0
$a^*_{10}m_1m_0$	0	0	0	0
$a^*_{11}m_1m_1$	0	$\frac{1}{2}(\sigma^{S^1})^2(x_1^\infty)^2$	0	0
$a^*_{12}m_1m_2$	0	0	0	0
$a^*_{20}m_2m_0$	0	0	0	0
$a^*_{21}m_2m_1$	0	0	0	0
$a^*_{22}m_2m_2$	0	0	0	$\frac{1}{2}(\sigma^{S^2})^2(x_2^\infty)^2$
$\sum_{i,j=0}^{1} a^*_{ij}m_im_j$	0	$\frac{1}{2}(\sigma^{S^1})^2(x_1^\infty)^2$	0	$\frac{1}{2}(\sigma^{S^2})^2(x_2^\infty)^2$
$a^*_{00,0}$	0	0	0	0
$a^*_{01,1}$	0	0	0	0
$a^*_{02,2}$	0	0	0	0
$a^*_{10,0}$	0	0	0	0
$a^*_{11,1}$	0	$(\sigma^{S^1})^2x_1^\infty$	$(\sigma^{S^1})^2x_1$	$(\sigma^{S^1})^2x_1$
$a^*_{12,2}$	0	$\frac{1}{2}\rho^{S^1S^2}\sigma^{S^1}\sigma^{S^2}x_1^\infty$	$\frac{1}{2}\rho^{S^1S^2}\sigma^{S^1}\sigma^{S^2}x_1$	$\frac{1}{2}\rho^{S^1S^2}\sigma^{S^1}\sigma^{S^2}x_1$
$a^*_{20,0}$	0	0	0	0
$a^*_{21,1}$	$\frac{1}{2}\rho^{S^1S^2}\sigma^{S^1}\sigma^{S^2}x_2$	$\frac{1}{2}\rho^{S^1S^2}\sigma^{S^1}\sigma^{S^2}x_2$	0	$\frac{1}{2}\rho^{S^1S^2}\sigma^{S^1}\sigma^{S^2}x_2^\infty$
$a^*_{22,2}$	$(\sigma^{S^2})^2x_2$	$(\sigma^{S^2})^2x_2$	0	$(\sigma^{S^2})^2x_2^\infty$
b_0^*	-1	-1	-1	-1
b_1^*	0	$(r^1-q^1)x_1^\infty$	$(r^1-q^1)x_1$	$(r^1-q^1)x_1$
b_2^*	$(r^2-q^2)x_2$	$(r^2-q^2)x_2$	0	$(r^2-q^2)x_2^\infty$
$(b_0^*-a^*_{0j,j})m_0$	0	0	0	0
$(b_1^*-a^*_{1j,j})m_1$	0	z_1	0	0
$(b_2^*-a^*_{2j,j})m_2$	0	0	0	z_2
$\sum_{i=0}^{2}(b_i^*-a^*_{ij,j})m_i$	0	z_1	0	z_2

$z_1 = ((\sigma^{S^1})^2 - r^1 + q^1 + \frac{1}{2}\rho^{S^1S^2}\sigma^{S^1}\sigma^{S^2})x_1^\infty$.
$z_2 = ((\sigma^{S^2})^2 - r^2 + q^2 + \frac{1}{2}\rho^{S^1S^2}\sigma^{S^1}\sigma^{S^2})x_2^\infty$.

References

[1] Brigo D, Morini M, Pallavicini A. Counterparty credit risk, collateral and funding with pricing cases for all asset classes. The Wiley Finance Series; 2013.
[2] Crépey S, Bielecki T. Counterparty risk and funding: A tale of two puzzles. Chapman and Hall–CRC Press; 2014.
[3] Gregory J. Counterparty credit risk and credit value adjustment. London: Wiley Finance; 2012.
[4] Piterbarg V. Funding beyond discounting: collateral agreements and derivatives pricing. Risk Mag 2010;2:97–102.
[5] Burgard C, Kjaer M. PDE representations of options with bilateral counterparty risk and funding costs. J Credit Risk 2011;7(3):1–19.
[6] García Muñoz LM. CVA, FVA (and DVA?) with stochastic spreads. A feasible replication approach under realistic assumptions. MPRA, 2013, http://mpra.ub.uni-muenchen.de/44568/.
[7] Arregui I, Salvador B, Vázquez C. PDE models and numerical methods for total value adjustment in European and American options with counterparty risk. Appl Math Comput 2017;308:31–53.
[8] Arregui I, Salvador B, Ševčovič D, Vázquez C. Total value adjustment for European options with two stochastic factors. Mathematical model, analysis and numerical simulation. Comput Math Appl 2018;76:725–40.
[9] Brigo D, Capponi A. Bilateral counterparty risk valuation with stochastic dynamical models and applications to CDSs. 2009, arXiv:0812.3705.
[10] Pallavicini A, Perini D, Brigo D. Funding, collateral and hedging: A consistent framework including CVA, DVA, collateral, netting rules and re-hypotecation. 2011, Available at https://ssrn.com/abstract=1969114.
[11] Arregui I, Salvador B, Vázquez C. A Monte Carlo approach to American options pricing including counterparty risk. Int J Comput Math 2019;96(11):2157–76.
[12] Arregui I, Leitao Á, Salvador B, Vázquez C. Efficient parallel Monte-Carlo techniques for pricing American options including counterparty credit risk. Int J Comput Math 2023.
[13] Borovykh A, Oosterlee CW, Pascucci A. Efficient XVA computation under local Lévy models. SIAM J Financ Math 2018;9(1):251–73.
[14] Crépey S. Bilateral counterparty risk under funding constraints–Part I: Pricing. Math Finance 2015;25:1–22.
[15] Crépey S. Bilateral counterparty risk under funding constraints–Part II: CVA. Math Finance 2015;25:23–50.
[16] García Muñoz LM, de Lope F, Palomar J. Pricing derivatives in the new framework: OIS discounting, CVA, DVA & FVA. MPRA, 2015, https://mpra.ub.uni-muenchen.de/62086.
[17] Arregui I, Simonella R, Vázquez C. Total value adjustment for European options in a multi-currency setting. Appl Math Comput 2022;413:126647.
[18] Simonella R, Vázquez C. XVA in a multi-currency setting with stochastic foreign exchange rates. Math Comput Simulation 2023;207:59–79.
[19] E W, Hutzenthaler M, Jentzen A, Kruse T. On multilevel Picard numerical approximations for high-dimensional nonlinear parabolic partial differential equations and high-dimensional backward stochastic differential equation. J Sci Comput 2019;79:1534–71.
[20] Kjaer M. Consistent XVA metrics part ii: Multicurrency. Bloomberg; 2017, http://ssrn.com/abstract=2932338.
[21] Brigo D, Dalessandro A, Neugebauer M, Triki F. A stochastic processes toolkit for risk management. 2008, arXiv preprint arXiv:0812.4210.
[22] Pascucci A. PDE and martingale methods in option pricing. Springer Science & Business Media; 2011.

[23] López-Salas JG, Vázquez C. PDE formulation of some SABR/LIBOR market models and its numerical solution with a sparse grid combination technique. Comput Math Appl 2018;75(5):1616–34.
[24] López-Salas JG, Rodríguez S, Vázquez C. AMFR-W numerical methods for solving high dimensional SABR/LIBOR PDE models. SIAM J Sci Comput 2021;43(1):B30–54.
[25] Pardoux E, Peng S. Backward stochastic differential equations and quasilinear parabolic partial differential equations. In: Stochastic partial differential equations and their applications (Charlotte, NC,1991). Lecture notes control inf. sci., vol. 176, Springer, Berlin; 1992, p. 200–17.
[26] Beck C, Hutzenthaler M, Jentzen A. On nonlinear Feynman-Kac formulas for viscosity solutions of semilinear parabolic partial differential equations. Stoch Dyn 2021;21(8):21500148.
[27] Duffy DJ. Finite difference methods in financial engineering. John Wiley & Sons; 2006.
[28] Brenner SC, Scott LR. The mathematical theory of finite element methods. Springer; 2008.
[29] Pironneau O. On the transport-diffusion algorithm and its application to Navier-Stokes equations. Numer Math 1982;38:309–32.
[30] Vázquez C. An upwind numerical approach for an American and European option pricing model. Appl Math Comput.
[31] Arregui I, Salvador B, Ševčovič D, Vázquez C. PDE models for American options with counterparty risk and two stochastic factors: mathematical analysis and numerical solution. Comput Math Appl 2020;79(5):1525–42.
[32] Fichera G. Problemi elastostatici con vincoli unilaterali: il problema di Signorini con ambigue condizioni al contorno. In: Atti della accademia nazionale dei lincei, ser. VII, vol. 7. 1964, p. 613–79.
[33] Oleĭnik OA, Radkevič EV. Second order equations with nonnegative characteristic form. New York, London: AMS, Plenum Press; 1973.
[34] D'Halluin Y, Forsyth PA, Labahn G. A semi–Lagrangian approach for American Asian options under jump-diffusion. SIAM J Sci Comput 2005;27:315–45.
[35] Castillo D, Ferreiro AM, García-Rodríguez JA, Vázquez C. Numerical methods to solve PDE models for pricing business companies in different regimes and implementation in GPUs. Appl Math Comput 2014;219:11233–57.
[36] Kloeden PE, Platen E. Numerical solution of stochastic differential equations. Berlin: Springer; 2011.
[37] Deelstra G, Delbaen F, et al. Convergence of discretized stochastic (interest rate) processes with stochastic drift term. Appl Stoch Models Data Anal 1998;14(1):77–84.
[38] Hutzenthaler M, Jentzen A, Kruse T, Nguyen T, von Wurstemberger P. Overcoming the curse of dimensionality in the numerical approximation of semilinear parabolic partial differential equations. Proc R Soc A 2020;476(2244):20190630.
[39] Heinrich S. Monte Carlo complexity of global solution of integral equation. J Complex 1998;14(2):151–75.
[40] Heinrich S. Multilevel Monte Carlo methods. In: International conference on large-scale scientific computing. Springer; 2001, p. 58–67.
[41] Giles M. Multilevel Monte Carlo path simulation. Oper Res 2008;56(3):607–17.
[42] Rapuch G, Roncalli T. Dependence and two-asset options pricing. J Comput Finance 2004;7(4):23–33.